

BAYESIAN D-OPTIMAL EXPERIMENTAL DESIGNS VIA COLUMN SUBSET SELECTION*

SRINIVAS ESWAR[†], VISHWAS RAO[‡], AND ARVIND K. SAIBABA[§]

Abstract. This paper tackles optimal sensor placement for Bayesian linear inverse problems, a popular version of the more general Optimal Experimental Design (OED) problem, using the D-optimality criterion. This is done by establishing connections between sensor placement and Column Subset Selection Problem (CSSP), which is a well-studied problem in Numerical Linear Algebra (NLA). In particular, we use the Golub-Klema-Stewart (GKS) approach which involves computing the truncated Singular Value Decomposition (SVD) followed by a pivoted QR factorization on the right singular vectors. The algorithms are further accelerated by using randomization to compute the low-rank approximation as well as for sampling the indices. The resulting algorithms are robust, computationally efficient, amenable to parallelization, require virtually no parameter tuning, and come with strong theoretical guarantees. One of the proposed algorithms is also adjoint-free which is beneficial in situations, where the adjoint is expensive to evaluate or is not available. Additionally, we develop a method for data completion without solving the inverse problem. Numerical experiments on model inverse problems involving the heat equation and seismic tomography in two spatial dimensions demonstrate the performance of our approaches.

Key words. Column Subset Selection Problem, Sensor Placement, Optimal Experimental Design, Bayesian inverse problems, Randomized algorithms.

MSC codes. 35R30, 62K05, 68W20, 65C60, 62F15

1. Introduction. Inverse problems involve reconstructing parameters describing mathematical models from the data. They have wide-ranging applications in medical imaging, geosciences, and other areas of science and engineering. The inverse problems we tackle are ill-posed and to address this, we use the Bayesian approach to inverse problems which produces a posterior distribution for the reconstruction by combining the likelihood and the prior distributions through the Bayes formula. The posterior distribution captures the uncertainty present in the reconstructions.

A central problem in Bayesian inverse problems is to determine how to optimally collect data. This falls under the umbrella of Optimal Experimental Design (OED). A common instance of OED is to determine the optimal location of a fixed number of sensors. The number of sensors and the locations they can be deployed in are limited due to budgetary and physical constraints. We consider the scenario that we have identified a set of m candidate sensor locations and each sensor contributes to one piece of information; given a budget of k sensors, find the best sensor locations. Put more plainly, choose k “best” sensors out of m . In OED, the notion of optimality is typically defined in terms of a criterion that quantifies the uncertainty in the reconstruction. In this paper, we focus on the D-optimality criterion which is the expected Kullback-Liebler divergence from the prior to the posterior distributions, and is a measure of information gain. For linear inverse problems with Gaussian priors, the D-optimal criterion has a closed-form expression that involves the determinant of the posterior covariance matrix.

* AKS was supported by the National Science Foundation through the award DMS-1845406 and the Department of Energy through the award DE-SC0023188. Vishwas Rao and Srinivas Eswar are supported by the U.S. Department of Energy, Office of Science, Advanced Scientific Computing Research Program under contracts DE-AC02-06CH11357 and DE-SC0023188.

[†]Mathematics and Computer Science Division, Argonne National Laboratory. seswar@anl.gov.

[‡]Mathematics and Computer Science Division, Argonne National Laboratory. vhebbur@anl.gov.

[§]Department of Mathematics, North Carolina State University. asaibab@ncsu.edu.

There are several challenges involved in sensor placement and OED. Choosing k out of m sensors involves potentially $\binom{m}{k}$ comparisons, which is infeasible even for modest values of m and k , and the optimal selected sensors may not even be unique. To compound these difficulties, even a single objective function evaluation is expensive since it requires many Partial Differential Equation (PDE) solves and in the case of the D-optimality criterion, involves expensive determinant computations. There are many approaches in the literature (reviewed in Section 2) to address these challenges.

In this paper, we take a radically different approach and view the problem through the lens of Column Subset Selection Problem (CSSP), which is a well-studied problem in NLA. To motivate the connection, we consider a matrix $\mathbf{A} \in \mathbb{R}^{n \times m}$ and consider the problem of choosing the “best” k columns of \mathbf{A} . As will be discussed in Section 2, each column of \mathbf{A} corresponds to a sensor. Motivated by this connection, we develop a computational framework for sensor placement using tools from CSSP with provable guarantees for the D-optimality criterion and the computational cost. The algorithms are very efficient and the cost is comparable to computing a truncated SVD of the forward operator preconditioned by the prior covariance matrix which is known to have low-rank. Our approach also suggests a method for data completion, i.e., filling in the missing values of the sensors at which data is not collected using the data that is actually collected. This data can be used by another inverse problem solution technique, e.g., filtered backpropagation. We briefly survey the contents of this paper and highlight our contributions.

Contributions and Features. This paper makes fundamental contributions to the theory and practice of D-optimal experimental design for Bayesian inverse problems. We summarize the main contributions of this paper and give a brief outline of the paper. Necessary background information is given in Section 2 including a review of the literature (Section 2.2).

1. **Connections to CSSP:** In Section 3, we interpret sensor placement for D-optimal experimental design through the lens of CSSP, a framework in NLA for selecting the “best” k columns out of m . We also draw connections to Rank-Revealing QR factorization (RRQR) and volume-maximization problems. The latter connection also allows us to establish that D-optimal sensor placement is NP-hard, and derive bounds on the performance of greedy algorithms.
2. **Algorithms:** The connection to CSSP allows us to develop many algorithms. The algorithms are based on the GKS framework and involve computation of the (truncated) SVD, followed by subset selection on the right singular vectors \mathbf{V}_k of a matrix \mathbf{A} (the details of this matrix are given in Section 2). The first set of algorithms uses pivoted QR on \mathbf{V}_k^T (Section 3.3). The second algorithm Randomized Adjoint-free OED (RAF-OED) (Section 4) is randomized and is adjoint-free and amenable to parallelization. The final set of algorithms (Section 5) uses randomized sampling and these approaches are cheaper than QR with Column Pivoting (QRCP). The proposed algorithms are computationally efficient and require no tuning or input from the user apart from the desired number of sensors k .
3. **Analysis:** All the proposed algorithms come with rigorous justification of the bounds on the D-optimality criterion. For the randomized sampling approaches, the bounds hold with high probability. We also provide detailed analyses of the computational cost with complexity estimates. The dominant computational cost is the computation of a truncated SVD of \mathbf{A} . Assuming each forward/adjoint operator evaluation is one PDE evaluation, the cost of

the proposed algorithms are $\sim 4k$ PDE solves (assuming randomized SVD with one subspace iteration), and RAF-OED only requires $\sim k$ PDE solves.

4. **Data completion:** In Section 6, we present an approach called Bayesian-Discrete Empirical Interpolation Method (B-DEIM) and show how the measured data can be used to estimate the data at the sensor locations at which data is not collected. We derive error analysis for the completed data and the error in the Maximum a posteriori (MAP) estimate using the completed data.
5. **Numerical experiments:** We perform detailed numerical experiments on model inverse problems involving recovering the initial condition from final time measurements, where the governing dynamics follow the heat equation and seismic tomography in two spatial dimensions. The experiments demonstrate the performance of our algorithms.

For ease of exposition, the proofs of the results are given in Section 7. Additional background and results are given in Section 9.

2. Preliminaries. This section reviews the notation used in this article and gives background information on Bayesian inverse problems, OED, and rank-revealing QR factorizations.

2.1. Notation and matrix preliminaries. Matrices are represented with bold uppercase letters like \mathbf{A} and vectors with bold lowercase letters like \mathbf{v} . Sets will be represented by uppercase letters like S . \mathbf{I}_n is the $n \times n$ identity matrix with \mathbf{e}_j as its j^{th} column. We denote a selection operator $\mathbf{S} = [\mathbf{e}_{i_1} \ \dots \ \mathbf{e}_{i_k}] \in \mathbb{R}^{n \times k}$, which contains columns from the identity matrix corresponding to the set of indices $S = \{i_1, \dots, i_k\}$. We also employ Matlab-style indexing to address elements of vectors and matrices. For example, $\mathbf{A}(:, S) = \mathbf{AS}$ selects the columns of \mathbf{A} indexed by the set S . The complete set of indices is denoted by $[n] = \{1, \dots, n\}$. The vector of all ones is represented as \mathbf{e} .

Let $\|\mathbf{x}\|_2$ denote the 2-norm for a vector \mathbf{x} and $\|\mathbf{A}\|_2$ denote the spectral norm for a matrix \mathbf{A} . If $\mathbf{M} \in \mathbb{R}^{n \times n}$ is positive definite, we define the weighted norm $\|\mathbf{x}\|_{\mathbf{M}} = \sqrt{\mathbf{x}^T \mathbf{M} \mathbf{x}}$. We use \log to denote the natural logarithm and $\text{logdet}(\mathbf{M}) \equiv \log(\det(\mathbf{M}))$, where $\det(\mathbf{M})$ denotes the determinant of the matrix \mathbf{M} . Let $\mathbf{C}, \mathbf{D} \in \mathbb{R}^{n \times n}$ be symmetric matrices. We say that $\mathbf{C} \preceq \mathbf{D}$ (alternatively, $\mathbf{D} \succeq \mathbf{C}$) if $\mathbf{D} - \mathbf{C}$ is positive semidefinite. This is known as Löwner partial ordering and additional properties are given in Appendix A.

The SVD of $\mathbf{A} \in \mathbb{R}^{n \times m}$ with $k \leq \text{rank}(\mathbf{A})$ is partitioned

$$(2.1) \quad \mathbf{A} = [\mathbf{U}_k \ \mathbf{U}_\perp] \begin{bmatrix} \boldsymbol{\Sigma}_k & \\ & \boldsymbol{\Sigma}_\perp \end{bmatrix} \begin{bmatrix} \mathbf{V}_k^T \\ \mathbf{V}_\perp^T \end{bmatrix},$$

where $\boldsymbol{\Sigma}_k \in \mathbb{R}^{k \times k}$ is invertible and contains the dominant singular values of \mathbf{A} , and matrices $\mathbf{U}_k \in \mathbb{R}^{n \times k}$ and $\mathbf{V}_k \in \mathbb{R}^{m \times k}$ have orthonormal columns and contain the corresponding left and right singular vectors respectively. Similarly, $\boldsymbol{\Sigma}_\perp$ contain the subdominant singular values with corresponding singular vectors in \mathbf{U}_\perp and \mathbf{V}_\perp respectively. For two matrices $\mathbf{A} \in \mathbb{R}^{m \times n}, \mathbf{B} \in \mathbb{R}^{n \times p}$ for which the product \mathbf{AB} is defined, we have the singular value inequalities [6, Problem III.6.2]

$$\sigma_j(\mathbf{AB}) \leq \sigma_j(\mathbf{A})\sigma_1(\mathbf{B}) \quad 1 \leq j \leq \min\{m, p\}.$$

2.2. Background on inverse problems and OED. Consider the measurement equation

$$(2.2) \quad \mathbf{d} = \mathbf{F}\mathbf{m} + \boldsymbol{\epsilon},$$

where $\mathbf{d} \in \mathbb{R}^m$ is the data, $\mathbf{F} \in \mathbb{R}^{m \times n}$ is the composition of the observation operator and the forward model. The vector \mathbf{m} is the parameter to be reconstructed and is a discretized representation of a spatially-dependent function, so it is very high-dimensional. We assume throughout this paper that $m < n$, that is, the problem is underdetermined. The vector $\boldsymbol{\epsilon}$ represents the observation noise, which we assume is Gaussian, that is, $\boldsymbol{\epsilon} \sim \mathcal{N}(0, \boldsymbol{\Gamma}_{\text{noise}})$. In the bulk of the paper, we consider the uncorrelated noise case $\boldsymbol{\Gamma}_{\text{noise}} = \eta^2 \mathbf{I}_m$. An extension to the case of a diagonal covariance matrix $\boldsymbol{\Gamma}_{\text{noise}}$ is straightforward, but we avoid this to simplify the exposition. An extension to the general uncorrelated case is left for future work. The inverse problem involves reconstructing the parameters \mathbf{m} from the measurements \mathbf{d} . We will be more specific about the measurements when we discuss OED.

As this is an ill-posed problem, a prevalent approach is to use the Bayesian paradigm [10, 45]. The Bayesian formulation of the inverse problem [48, 38, 51, 50] first determines the prior information, which in our paper we take to be Gaussian $\mathbf{m} \sim \mathcal{N}(\boldsymbol{\mu}_{\text{pr}}, \boldsymbol{\Gamma}_{\text{pr}})$. Then using Bayes' rule, we derive an expression for the posterior distribution with density $\pi_{\text{post}}(\mathbf{m}|\mathbf{d})$

$$\begin{aligned} \pi_{\text{post}}(\mathbf{m}|\mathbf{d}) &= \frac{\pi_{\text{like}}(\mathbf{d}|\mathbf{m})\pi_{\text{pr}}(\mathbf{m})}{\pi(\mathbf{d})}, \\ &\propto \exp\left(-\frac{1}{2}\|\mathbf{d} - \mathbf{F}\mathbf{m}\|_{\boldsymbol{\Gamma}_{\text{noise}}^{-1}}^2 - \frac{1}{2}\|\mathbf{m} - \boldsymbol{\mu}_{\text{pr}}\|_{\boldsymbol{\Gamma}_{\text{pr}}^{-1}}^2\right). \end{aligned}$$

Under the assumptions made thus far, the posterior distribution is Gaussian of the form $\mathcal{N}(\mathbf{m}_{\text{post}}, \boldsymbol{\Gamma}_{\text{post}})$, where the covariance matrix $\boldsymbol{\Gamma}_{\text{post}} \equiv (\mathbf{F}^T \boldsymbol{\Gamma}_{\text{noise}}^{-1} \mathbf{F} + \boldsymbol{\Gamma}_{\text{pr}}^{-1})^{-1}$ and the posterior mean is

$$(2.3) \quad \mathbf{m}_{\text{post}} \equiv \boldsymbol{\Gamma}_{\text{post}}(\mathbf{F}^T(\boldsymbol{\Gamma}_{\text{noise}}^{-1} \mathbf{d}) + \boldsymbol{\Gamma}_{\text{pr}}^{-1} \boldsymbol{\mu}_{\text{pr}}).$$

We consider the sensor placement problem which is one flavor of OED. See [53, 43, 1, 15] for good introductions to this topic. In this version of the problem, there are m candidate sensor locations $\{\mathbf{x}_1, \dots, \mathbf{x}_m\}$, at which we can consider placing the sensor. But due to budgetary or physical considerations, we can only deploy k sensors and, thus, we would like to pick the ‘‘best’’ k locations, out of m , to place our sensors. This can be encoded as a set of indices $S = \{i_1, \dots, i_k\}$ indicating the selected sensors. To determine the optimal sensor locations we solve the optimization problem

$$(2.4) \quad \min_S \phi(S), \text{ subject to } |S| \leq k.$$

Here $\phi(S)$ is an objective function determining sensor placement and S is the set of $\binom{m}{k}$ indices. This is a constrained binary optimization problem for determining the sensor locations. Popular criteria for OED selection are the Bayesian A-optimality criterion and the D-optimality criterion which, for linear inverse problems, amounts to computing the trace and log-determinant of the posterior covariance matrices. In this paper, we focus on the D-optimal criterion, which measures the information gain from the prior to the posterior distribution; equivalently, it is the expected Kullback-Liebler divergence from the prior to the posterior distributions [2]. For the present

problem setting, the criterion takes the form

$$(2.5) \quad \phi(S) = \log\det(\mathbf{I} + \mathbf{A}(:, S)\mathbf{A}(:, S)^\top),$$

where the matrix \mathbf{A} is given by

$$(2.6) \quad \mathbf{A} \equiv \mathbf{\Gamma}_{\text{pr}}^{1/2} \mathbf{F}^\top \mathbf{\Gamma}_{\text{noise}}^{-1/2} \in \mathbb{R}^{n \times m}.$$

For simplicity of notation, we define

$$(2.7) \quad \Psi(\mathbf{G}) \equiv \log\det(\mathbf{I} + \mathbf{G}\mathbf{G}^\top),$$

so that $\phi(S) = \Psi(\mathbf{A}(:, S))$.

The columns of \mathbf{A} correspond to the m sensors, and selecting k columns is tantamount to selecting sensors. This is the key insight that we exploit in this article. Throughout this paper we will assume that the number of sensors k is smaller than the rank of \mathbf{A} . Note that the D-optimality criterion can be expressed in terms of the posterior and the prior covariance matrices as $\phi([m]) = \Psi(\mathbf{A}) = -\log\det(\mathbf{\Gamma}_{\text{post}}) + \log\det(\mathbf{\Gamma}_{\text{pr}})$.

Challenges and related work. There are several challenges associated with OED: first, forming the posterior covariance matrix explicitly is infeasible, so even a single evaluation of these OED criteria is infeasible, and second, the optimization over the set of sensors is a constrained binary optimization problem which is challenging to solve. A detailed review of OED and its challenges is outside the scope of this paper, but further details can be found in [15, 1, 36].

To tackle the first challenge, one can use randomized techniques to efficiently evaluate the objective functions, which we also adopt in this paper. There are several strategies to address the second challenge. One approach is to use greedy approaches in which we sequentially select the next best sensor location given a current selection of sensors. Greedy approaches are popular when it comes to sensor placement since they are relatively simple to implement but are typically suboptimal. Justifications for greedy approaches typically rely on the connection to super-modularity (or sub-modularity), see e.g., [1, Section 4.8] and [37]. Another approach is to relax the optimization problem to a continuous optimization problem (see, e.g., [30]) with an appropriate regularization term to enforce sparsity. The continuous optimization problem is then solved using gradient-based optimization techniques. Finally, the optimized weights are then thresholded to obtain binary designs. Related to this approach, a method that avoided the use of adjoints was proposed in [33, Chapter 5]; see also [1, Section 4.5]. Another recent approach involves interpreting the binary designs as Bernoulli random variables and expressing the objective function as an expectation, thus allowing the use of stochastic optimization techniques [3].

In contrast to the previous approaches, this article takes a fresh perspective by viewing OED as a problem of selecting k columns from \mathbf{A} out of m . This allows us to adapt existing techniques for CSSP, including high-quality software implementations, to OED. The resulting algorithms are efficient, robust, and require virtually no parameter tuning. The performance of the algorithms comes with strong theoretical guarantees. The algorithms rely on low-rank computations of \mathbf{A} which are accelerated using randomized techniques. The closest works to ours are [57, 58], which also exploit low-rank approximations and swapping algorithms based on leverage scores, but these papers do not explore the connections to CSSP and give theoretical guarantees.

Other related work. While not directly related to OED, the notion of algorithmic leveraging [39] is used to subsample (and then appropriately scale) the data sets and matrices to reduce the computational cost. For example, leverage score-based methods have been used to provide scalable regression estimators via sampling [59, 39]. Similarly, a related approach for data reduction is in [55]. However, in contrast, OED typically seeks to reduce data because of physical or budgetary constraints, rather than computational considerations. Another difference compared to the previous approaches is that they do not address the Bayesian setting, which is the focus of this paper. CSSP methods have applications beyond compressing a matrix by selecting a subset of its columns [27]. It has been used for clustering [9], data analysis [40], feature selection [7], multipoint boundary value problems [19, 20], image applications [14], graph signal processing [52], among others. These works only mention OED in passing and do not establish the various connections to CSSP as in this work.

2.3. Rank-revealing QR factorizations. The pivoted QR factorization of a matrix $\mathbf{M} \in \mathbb{R}^{m \times n}$ with $m \geq n$ with $\text{rank}(\mathbf{M}) = k \leq n$ is

$$(2.8) \quad \mathbf{M}\mathbf{\Pi} = \mathbf{Q}\mathbf{R} = [\mathbf{Q}_1 \quad \mathbf{Q}_2] \begin{bmatrix} \mathbf{R}_{11} & \mathbf{R}_{12} \\ & \mathbf{R}_{22} \end{bmatrix},$$

where $\mathbf{Q} \in \mathbb{R}^{m \times m}$ is orthogonal, $\mathbf{R}_{11} \in \mathbb{R}^{k \times k}$ is upper triangular with nonnegative diagonal elements, $\mathbf{R}_{12} \in \mathbb{R}^{k \times (n-k)}$, $\mathbf{R}_{22} \in \mathbb{R}^{(m-k) \times (n-k)}$, and $\mathbf{\Pi} \in \mathbb{R}^{n \times n}$ is a permutation matrix. The aim is to select a permutation matrix that separates the linearly dependent columns of \mathbf{M} from the linearly independent ones. This notion was made more precise in Gu and Eisenstat [29].

A factorization is called a *Strong Rank-Revealing QR factorization* (sRRQR) if it satisfies the following criteria (for $1 \leq i \leq j$ and $1 \leq j \leq n - k$)

$$(2.9) \quad \sigma_i(\mathbf{M}) \geq \sigma_i(\mathbf{R}_{11}) \geq \frac{\sigma_i(\mathbf{M})}{p_1(k, n)} \quad \text{and} \quad \sigma_{k+j}(\mathbf{M}) \leq \sigma_j(\mathbf{R}_{22}) \leq \sigma_{k+j}(\mathbf{M}) p_1(k, n)$$

and

$$(2.10) \quad \left| (\mathbf{R}_{11}^{-1} \mathbf{R}_{12})_{ij} \right| \leq p_2(k, n),$$

for $1 \leq i \leq k$ and $1 \leq j \leq n - k$ [29]. Here $p_1(k, n)$ and $p_2(k, n)$ are functions bounded by low-degree polynomials in k and n . The upper bound for \mathbf{R}_{11} and lower bound for \mathbf{R}_{22} hold for any pivoted QR factorization because of interlacing inequalities. Gu and Eisenstat [29] present algorithms that, given $f \geq 1$, find a $\mathbf{\Pi}$ for which (2.9) and (2.10) hold with

$$(2.11) \quad p_1(k, n) = \sqrt{1 + f^2 k(n - k)} \quad \text{and} \quad p_2(k, n) = f.$$

When $f > 1$, these methods take $O((m + n \log_f n) n^2)$ floating point operations (flops). This reduces to $O(mn^2)$ flops when f is a small power of n . For the short and wide case, i.e. where $m < n$, the operation count is $O(m^2 n \log_f n)$ flops [4].

While the asymptotic complexity of sRRQR is similar to that of standard QR factorization, it is considerably more complicated to implement efficiently on modern computers. This is because the best permutation order does not have an optimal substructure, i.e., the order for the best k columns need not contain all of the best $k - 1$ columns. Therefore, a lot of column swapping occurs hurting the efficiency of such algorithms.

The popular QRCP was first introduced by Businger and Golub to find a Rank-Revealing QR factorization [13]. It is a simple modification of the ordinary QR factorization, where at every step the column with the largest norm in \mathbf{R}_{22} is pivoted to the front and orthogonalized. QRCP takes about $4mnk - 2k^2(m+n) + 4k^3/3$ flops and is a standard function in many linear algebra packages [44]. This algorithm works well in practice, but there are examples where it fails to satisfy (2.9) and (2.10). In the worst case, QRCP may achieve exponential bounds with $p_1(k, n) = \sqrt{n-k} \cdot 2^k$ and $p_2(k, n) = 2^{k-1}$ [29].

3. Column subset selection for OED. In Section 3.1, we first give an interpretation of sensor placement in terms of CSSP. We give bounds for the D-optimality criterion in Section 3.2 which motivates the algorithms in Section 3.3.

3.1. Interpreting OED as CSSP. Consider the matrix $\mathbf{A} \in \mathbb{R}^{n \times m}$ and recall that the columns of \mathbf{A} correspond to the number of design variables (e.g., sensors). We argue that finding the “best” k sensors out of m is closely related to identifying k “best” columns of \mathbf{A} . The D-optimal criterion seeks to maximize

$$(3.1) \quad \phi(S) \equiv \Psi(\mathbf{C}) = \log \det(\mathbf{I} + \mathbf{C}\mathbf{C}^\top)$$

over the set of all matrices \mathbf{C} (containing columns from \mathbf{A} indexed by the set S with $|S| = k$ such that $\mathbf{C} = \mathbf{A}(:, S)$; alternatively all $m \times m$ permutation matrices $\mathbf{\Pi}$ such that $\mathbf{C} = \mathbf{A}\mathbf{\Pi}(:, 1:k)$). We will discuss interpretations in terms of maximum-volume, RRQR, and GKS approaches; the algorithms we develop are in the GKS framework.

Connection to maximum-volume. A related problem in NLA is finding the submatrix of a matrix with maximum volume, which was shown to be an NP-hard problem [18]. Given a matrix $\mathbf{M} \in \mathbb{R}^{n \times m}$, the volume of a matrix is the volume of the n -dimensional parallelepiped formed by the columns of \mathbf{M} ; it has the following explicit formulas

$$\text{vol}(\mathbf{M}) \equiv \sqrt{\det(\mathbf{M}^\top \mathbf{M})} = \prod_{j=1}^{\min\{m,n\}} \sigma_j(\mathbf{M}).$$

To see the connection to the maximum volume submatrix problem, observe that by the Sylvester determinant identity

$$\det(\mathbf{I} + \mathbf{A}\mathbf{A}^\top) = \det(\mathbf{I} + \mathbf{A}^\top \mathbf{A}) = \det\left(\begin{bmatrix} \mathbf{I} & \mathbf{A}^\top \\ \mathbf{A} & \mathbf{0} \end{bmatrix}\right) = \text{vol}\left(\begin{bmatrix} \mathbf{I} \\ \mathbf{A} \end{bmatrix}\right)^2.$$

That is, solving the D-optimal optimization problem is a special case of maximum-volume estimation which is known to be NP-hard ([18, Theorem 4]). However, that does not readily establish that D-optimal sensor placement is NP-Hard but we give a proof for the sake of completion. On the other hand, classical OED is known to be NP-hard [56].

PROPOSITION 3.1. *The optimization problem of optimizing the objective function (3.1) over all index sets S corresponding to k columns from \mathbf{A} is NP-hard.*

Proof. The proof is an extension of the proof technique of [18, Theorem 4] and is, therefore, relegated to Appendix B. \square

This connection to maximum volume can also be used to develop a greedy selection approach to maximize $\text{vol}(\begin{bmatrix} \mathbf{I} & \mathbf{A}^\top \end{bmatrix})$. The details of this approach are given in [18, Algorithm 1]. It can be shown via [18, Theorem 11] that the selected columns S satisfy

$$\phi(S) \leq \phi(S^{\text{opt}}) \leq 2 \log(k!) + \phi(S).$$

Here, S^{opt} denotes the index set corresponding to an optimal set of columns (recall this is not unique). We give some alternative approaches based on maximum-volume in Appendix C.2.

Connection to RRQR. To understand the connection of sensor placement to RRQR, consider the pivoted QR factorization of \mathbf{A}

$$\mathbf{A} [\mathbf{\Pi}_1 \quad \mathbf{\Pi}_2] = [\mathbf{C} \quad \mathbf{T}] = [\mathbf{Q}_1 \quad \mathbf{Q}_2] \begin{bmatrix} \mathbf{R}_{11} & \mathbf{R}_{12} \\ & \mathbf{R}_{22} \end{bmatrix}.$$

From the relation $\mathbf{C} = \mathbf{Q}_1 \mathbf{R}_{11}$, it is easy to see that

$$\log \det(\mathbf{I} + \mathbf{C}\mathbf{C}^\top) = \log \det(\mathbf{I}_k + \mathbf{R}_{11} \mathbf{R}_{11}^\top).$$

Therefore, this relation shows that maximizing $\log \det(\mathbf{I} + \mathbf{C}\mathbf{C}^\top)$ is the same as maximizing $\log \det(\mathbf{I}_k + \mathbf{R}_{11} \mathbf{R}_{11}^\top)$. The sRRQR algorithm attempts to maximize $\det(\mathbf{R}_{11})$ by interchanging the most “dependent” column of \mathbf{R}_{11} (from index $1 \leq i \leq k$), or the most independent column of \mathbf{R}_{22} (index $k+1 \leq i \leq n$). It may be possible to modify sRRQR to instead search for a maximizer of $\log \det(\mathbf{I}_k + \mathbf{R}_{11} \mathbf{R}_{11}^\top)$. However, we did not pursue this approach. One reason is that the sRRQR approach implicitly assumes that the entries of \mathbf{A} are available explicitly. But in the applications we consider, we can only perform matrix-vector products (matvecs) with \mathbf{A} (and \mathbf{A}^\top), so we need to use matrix-free approaches.

The Golub-Klema-Stewart (GKS) approach. Instead of RRQR, we follow the GKS approach, which has two stages. In the first stage, a truncated SVD of $\mathbf{A} \approx \mathbf{U}_k \mathbf{\Sigma}_k \mathbf{V}_k^\top$ is computed, where $\mathbf{V}_k \in \mathbb{R}^{m \times k}$ contains the right singular vectors corresponding to the largest singular values of \mathbf{A} . In the second stage, we partition \mathbf{V}_k^\top as

$$(3.2) \quad \mathbf{V}_k^\top [\mathbf{\Pi}_1 \quad \mathbf{\Pi}_2] = [\mathbf{V}_{11} \quad \mathbf{V}_{12}].$$

Here $\mathbf{\Pi}_1 \in \mathbb{R}^{n \times k}$ and we define $\mathbf{C} = \mathbf{A}\mathbf{\Pi}_1$. Assuming that \mathbf{V}_{11} is nonsingular, it can be shown that [26, Theorem 5.5.2]

$$\frac{\sigma_k(\mathbf{A})}{\|\mathbf{V}_{11}^{-1}\|_2} \leq \sigma_k(\mathbf{C}) \leq \sigma_k(\mathbf{A}).$$

Thus, the smallest singular value of $\sigma_k(\mathbf{C})$ is close to $\sigma_k(\mathbf{A})$, except for the factor $\|\mathbf{V}_{11}^{-1}\|_2$. The lower bound clearly identifies the factor $\|\mathbf{V}_{11}^{-1}\|_2$; since \mathbf{V}_{11}^\top is an invertible submatrix of \mathbf{V}_k it follows that $\|\mathbf{V}_{11}^{-1}\|_2 \geq 1$. Therefore, one goal is to identify a permutation matrix $\mathbf{\Pi}$ such that $\|\mathbf{V}_{11}^{-1}\|_2$ is as close to 1 as possible; in other words, we want to find a set of k well-conditioned columns of \mathbf{V}_k^\top . This analysis casts light only on the smallest singular value of \mathbf{C} but the D-optimality criterion involves all the singular values of \mathbf{C} , which we address in the next section. In contrast to RRQR, GKS works with the truncated SVD which can be computed in a matrix-free manner and this is more suitable to applications involving PDEs.

3.2. Structural bounds on the D-optimality of \mathbf{C} . We now derive bounds for the D-optimal criterion, when the columns $\mathbf{C} = \mathbf{A}\mathbf{\Pi}_1 = \mathbf{A}(:, S)$ have been computed using the GKS approach.

THEOREM 3.2. *Let $\mathbf{A} \in \mathbb{R}^{n \times m}$ with $k \leq \text{rank}(\mathbf{A})$. Then for any permutation $\mathbf{\Pi}$ such that $\text{rank}(\mathbf{V}_{11}) = k$ and $\mathbf{C} = \mathbf{A}\mathbf{\Pi}_1 = \mathbf{A}(:, S)$ we have,*

$$\Psi(\mathbf{\Sigma}_k / \|\mathbf{V}_{11}^{-1}\|_2) \leq \phi(S) \leq \phi(S^{\text{opt}}) \leq \Psi(\mathbf{\Sigma}_k) \leq \phi([m]).$$

Proof. See Section 7.1. □

As before, S^{opt} denotes the indices corresponding to an optimal set of columns and note that $\phi([m]) = \Psi(\mathbf{A}) = \log\det(\mathbf{I} + \mathbf{A}\mathbf{A}^\top)$.

We now discuss the interpretation of the bounds. First, consider the bounds $\phi(S^{\text{opt}}) \leq \Psi(\Sigma_k) \leq \phi([m])$, which says that the performance of “the best” set of columns in terms of the D-optimal criterion depends on the top- k singular values. More precisely, if the singular values don’t decay rapidly or the matrix is not approximately rank- k , then we cannot expect $\phi(S^{\text{opt}})$ to be close to $\phi([m])$. In other words, the upper bound is dictated by the singular value decay. On the other hand, consider the lower bound $\Psi(\Sigma_k/\|\mathbf{V}_{11}^{-1}\|_2) = \log\det(\mathbf{I} + \Sigma_k^2/\|\mathbf{V}_{11}^{-1}\|_2^2) \leq \phi(S)$. The lower bound clearly identifies the factor $\|\mathbf{V}_{11}^{-1}\|_2$ and as mentioned earlier, the goal is to identify a permutation matrix $\mathbf{\Pi}$ such that $\|\mathbf{V}_{11}^{-1}\|_2$ is as close to 1 as possible; in other words, we want to find a set of well-conditioned columns of \mathbf{V}_k^\top . We show below in Corollary 3.3 that sRRQR can be used to identify such a set of columns.

3.3. Deterministic CSSP algorithm for OED. In this section, we discuss implementation issues related to the OED computed using the GKS framework. There are two main computational issues to be addressed: first, the computation of the truncated SVD, and second, the cost of computing the permutation matrix for which we use pivoted QR. The details of the algorithm are given in Algorithm 3.1.

Bounds using pivoted QR. We consider the case that pivoted QR is used to compute the permutation matrix $\mathbf{\Pi}$. The result below quantifies the D-optimal criterion if sRRQR is used in Algorithm 3.1.

COROLLARY 3.3. *Suppose we select k columns from \mathbf{A} , denoted by the set S by applying sRRQR to \mathbf{V}_k^\top with factor $f \geq 1$. Let $q_f(m, k) \equiv \sqrt{1 + f^2k(m - k)}$. Then*

$$\Psi(\Sigma_k/q_f(m, k)) \leq \phi(S) \leq \phi(S^{\text{opt}}) \leq \Psi(\Sigma_k) \leq \phi([m]).$$

Proof. Follows from [23, Lemma 2.1] applied to \mathbf{V}_k^\top and Theorem 3.2. □

In particular, this result shows that the algorithm can find a set of columns that satisfy

$$(3.3) \quad \Psi(\Sigma_k/\sqrt{1 + k(m - k)}) \leq \phi(S) \leq \Psi(\Sigma_k) \leq \phi([m]),$$

but such a set of columns may take exponential time to compute.

Instead of sRRQR, we use QRCP in practice to compute the permutation matrix $\mathbf{\Pi}$. While the worst-case behavior for QRCP involves the factor $q(m, k) \leq \sqrt{m - k} 2^k$, the algorithm behaves remarkably well in practice. Furthermore, efficient implementations are available from LAPACK [44].

Computational cost. We perform a truncated SVD of the preconditioned forward operator to obtain the first k right singular vectors \mathbf{V}_k . This will require $\sim k$ applications of the forward and adjoint model each if we employ a matrix-free method for the SVD such as a Krylov subspace method [26] or Randomized SVD [31]. In numerical experiments, we use Randomized SVD to accelerate the computational cost with a Gaussian random matrix [31, Algorithm 5.1]. This results in a cost of

$$T_{\text{SVD}} \equiv 2\ell T_{\mathbf{A}} + O(k^2(m + n) + k^3) \text{ flops.}$$

Here $T_{\mathbf{A}}$ is the cost of a matvecs with \mathbf{A} or \mathbf{A}^\top and $\ell = k + p$ where $p \leq 20$ is the oversampling amount. For additional accuracy, we may also use Randomized SVD with subspace iterations, for some additional computational cost [31, Algorithm 5.2].

The running time for Algorithm 3.1 with sRRQR is $T_{\text{SVD}} + O(k^2 m \log_f m)$ flops (or $T_{\text{SVD}} + O(k^2 m)$ flops for QRCP). The matvecs with \mathbf{A} and \mathbf{A}^\top can be parallelized, leading to additional computational benefits.

Algorithm 3.1 OED via Deterministic CSSP

1: **procedure** GKS

Input: $\mathbf{F} \in \mathbb{R}^{m \times n}$, prior covariance matrix $\mathbf{\Gamma}_{\text{pr}}$, noise variance η^2 , and number of columns k .

Output: Set S such that $\mathbf{C} = \mathbf{A}(:, S) \in \mathbb{R}^{n \times k}$.

2: Define operator $\mathbf{A} = \eta^{-1} \mathbf{\Gamma}_{\text{pr}}^{1/2} \mathbf{F}^\top$.

3: Compute the truncated SVD: $[\tilde{\sim}, \tilde{\sim}, \mathbf{V}_k] = \text{svd}(\mathbf{A}, k)$.

4: Run pivoted QR: $[\tilde{\sim}, \tilde{\sim}, \mathbf{\Pi}] = \text{qr}(\mathbf{V}_k^\top)$.

5: Form S with the first k columns of $\mathbf{\Pi}$: $\mathbf{\Pi}_1 = \mathbf{\Pi}(:, 1 : k)$.

6: **end procedure**

4. RAF-OED approach. In this section, we develop an algorithm for OED called RAF-OED that is based on the approach described in Section 3.

In this approach, we draw a random matrix $\mathbf{\Omega} \in \mathbb{R}^{d \times n}$ which is a random embedding. For instance, we can draw $\mathbf{\Omega}$ as a Gaussian random matrix with independent entries drawn from $\mathcal{N}(0, 1/d)$. Next we form the sketch $\mathbf{Y} = \mathbf{\Omega} \mathbf{A} \in \mathbb{R}^{d \times m}$, which has the same number of columns as \mathbf{A} . We then perform subset selection on \mathbf{Y} by performing pivoted QR directly on \mathbf{Y} . This is described in Algorithm 4.1. Justification for this approach of subset selection is given in [54, 21, 24]. Other choices for the random matrix $\mathbf{\Omega}$ are possible and discussed in [41, Sections 8-9].

Algorithm 4.1 OED via RAF-OED

1: **procedure** RAF-OED

Input: $\mathbf{F} \in \mathbb{R}^{m \times n}$, prior covariance matrix $\mathbf{\Gamma}_{\text{pr}}$, noise variance η^2 , number of columns k , and oversampling parameter p .

Output: Set S such that $\mathbf{C} = \mathbf{A}(:, S) \in \mathbb{R}^{n \times k}$.

2: Draw random matrix $\mathbf{\Omega} \in \mathbb{R}^{d \times n}$, where $d = k + p$, with independent entries drawn from the distribution $\mathcal{N}(0, 1/d)$.

3: Define operator $\mathbf{A} = \mathbf{\Gamma}_{\text{pr}}^{1/2} \mathbf{F}^\top \eta^{-1}$ and compute $\mathbf{Y} = \mathbf{\Omega} \mathbf{A}$.

4: Run pivoted QR: $[\tilde{\sim}, \tilde{\sim}, \mathbf{\Pi}] = \text{qr}(\mathbf{Y})$.

5: Form S with the first k columns of $\mathbf{\Pi}$: $\mathbf{\Pi}_1 = \mathbf{\Pi}(:, 1 : k)$.

6: **end procedure**

A result similar to Theorem 3.2 and Corollary 3.3 can be stated for Algorithm 4.1.

THEOREM 4.1 (RAF-OED). *Let $d = k + p$ with $p \geq 2$ and let $\mathbf{\Pi}_1$ be the output of Algorithm 4.1 computed using sRRQR with $f \geq 1$. With probability at least $1 - \delta$*

$$\Psi(\mathbf{\Sigma}_k / (q_f^R(m, k) C_g)) \leq \phi(S) \leq \phi(S^{\text{opt}}) \leq \Psi(\mathbf{\Sigma}_k) \leq \phi([m]),$$

where $C_g \equiv \frac{\epsilon \sqrt{d}}{p+1} \left(\frac{2}{\delta}\right)^{1/(p+1)} (\sqrt{n} + \sqrt{d} + \sqrt{2 \log(2/\delta)})$.

Proof. See Section 7.2. □

Computational cost. Algorithm 4.1 requires $dT_{\mathbf{A}}$ matvecs with \mathbf{A} and an additional $\mathcal{O}(dm \min\{d, m\})$ flops. The value of d can be chosen either as $d = k + p$, where p is a small oversampling parameter. For more robust numerics, the choice of $d = 2k + 1$ might be appropriate. A remarkable aspect of this approach is that it only requires matvecs with \mathbf{A}^T ; that is, a matvec each with \mathbf{F} and $\mathbf{\Gamma}_{pr}^{1/2}$. Importantly, this completely avoids computing matvecs with \mathbf{F}^T . This property is valuable in applications in which adjoint computations with \mathbf{F} are either very expensive or not possible (for example, because of the use of legacy codes). Furthermore, the computations of matvecs with \mathbf{A} can be done in parallel, increasing the computational attractiveness of this method. Computing the MAP estimate in (2.3) may still require computing adjoints with \mathbf{F} , but this can be avoided using alternative techniques such as [42].

5. Randomized subset selection. Recall that the sRRQR algorithm takes $\mathcal{O}(k^2 m \log_f m)$ flops to select k columns from m , while QRCP costs $\mathcal{O}(k^2 m)$ flops. To further reduce this cost we use randomized sampling techniques. This approach involves sampling $s \geq k$ columns using a discrete probability distribution defined based on \mathbf{V}_k . The computational cost of sampling is $\mathcal{O}(km)$ which is attractive. The trade-off, however, is that we need to select $s \sim k \log k$ samples. Since we need to select exactly k columns (k sensors), we propose a hybrid approach (Section 5.1) that uses both randomization and pivoted QR factorizations to select columns efficiently. We discuss the analysis in Section 5.2, and a discussion of computational costs in Section 5.3.

5.1. Sampling algorithms. The *leverage score* sampling is a well-known approach for column subset selection (see e.g., [40, 4]). We first compute the right singular vectors \mathbf{V}_k and define the (subspace) leverage scores as $\tau_j = \|\mathbf{e}_j^T \mathbf{V}_k\|_2^2$ for $1 \leq j \leq m$ which are the squared row norms of \mathbf{V}_k . Note that since $\sum_{j=1}^m \tau_j = \|\mathbf{V}_k\|_F^2 = k$, the leverage scores can be used to define a probability distribution on $\{1, \dots, m\}$ with the probability of sampling index j as τ_j/k .

We define the sampling probabilities

$$(5.1) \quad \pi_j = \frac{\tau_j}{2k} + \frac{1}{2m} \quad 1 \leq j \leq m,$$

which is an average of the leverage score-based distribution and the uniform distribution. The idea is to handle cases where τ_j is almost zero and to ensure that π_j have nontrivial lower bounds [46]. Note that other distributions, such as $\pi_j = p_j / (\sum_{j=1}^m p_j)$, where $p_j = \max(\tau_j, k/m)$, for $1 \leq j \leq m$ can also be used instead which achieve similar bounds [4, Section 3.4]. Another option is to use a mixing parameter $\beta \in (0, 1]$ and take the convex combination of the leverage score and the uniform distributions $\pi_j^\beta = \beta \frac{\tau_j}{k} + (1 - \beta) \frac{1}{m}$ for $1 \leq j \leq m$.

The hybrid approach as described in Algorithm 5.1, works in two stages to return exactly k columns of \mathbf{A} . In the first stage, it generates $s = \mathcal{O}(k \log k)$ columns of \mathbf{A} chosen based on the probabilities $\{\pi_j\}_{j=1}^m$ chosen independently and with replacement. The method returns an appropriately weighted set of columns

$$(5.2) \quad \widehat{\mathbf{C}}_{\text{lev}} \equiv \mathbf{ASD} \in \mathbb{R}^{n \times s}.$$

Because we are sampling with replacement, repetition of the columns is allowed. The reason for weighting the columns is to ensure that $\mathbb{E}[(\mathbf{ASD})(\mathbf{ASD})^T] = \mathbf{AA}^T$ where the expectation is over the sampled indices [22, Lemma 3]. Similar ideas to the hybrid approach have been proposed earlier in [8, 11].

To further pare $\widehat{\mathbf{C}}_{\text{lev}}$ down to k columns, we perform sRRQR on $\mathbf{V}_k^T \mathbf{S} \mathbf{D}$ to obtain the selection operator $\mathbf{\Pi}_1 \in \mathbb{R}^{s \times k}$. The corresponding weighted columns of \mathbf{A} are

$$(5.3) \quad \widehat{\mathbf{C}}_{\text{hyb}} \equiv \widehat{\mathbf{C}}_{\text{lev}} \mathbf{\Pi}_1 = \mathbf{A} \mathbf{S} \mathbf{D} \mathbf{\Pi}_1 \in \mathbb{R}^{n \times k}.$$

The final selected indices correspond to the columns of $\mathbf{S} \mathbf{\Pi}_1 \in \mathbb{R}^{m \times k}$ and the corresponding selected columns of \mathbf{A} are $\mathbf{C}_{\text{hyb}} \equiv \mathbf{A} \mathbf{S} \mathbf{\Pi}_1 = \mathbf{A}(:, S_{\text{hyb}})$.

A precise analysis of the minimal number of samples is given shortly.

Algorithm 5.1 OED via randomized sampling

1: **procedure** RANDOMSAMPLING

Input: $\mathbf{F} \in \mathbb{R}^{m \times n}$, prior covariance matrix $\mathbf{\Gamma}_{\text{pr}}$, noise variance η^2 , number of columns k , number of samples $s \geq k$.

Output: Set S such that $\mathbf{C} = \mathbf{A}(:, S) \in \mathbb{R}^{n \times k}$.

2: Define operator $\mathbf{A} = \eta^{-1} \mathbf{\Gamma}_{\text{pr}}^{1/2} \mathbf{F}^T$.

3: Compute the truncated SVD: $[\sim, \sim, \mathbf{V}_k] = \text{svd}(\mathbf{A}, k)$.

4: Compute the leverage scores in (5.1).

5: Stage 1: Generate s indices $\{i_1, \dots, i_s\}$ from $\{1, \dots, m\}$ with probabilities $\{\pi_j\}_{j=1}^m$ independently and with replacement.

6: Define the selection operator $\mathbf{S} = [\mathbf{e}_{i_1} \ \dots \ \mathbf{e}_{i_s}]$ and weights

$$\mathbf{D} = \text{diag} \left(\frac{1}{\sqrt{s\pi_{i_1}}}, \dots, \frac{1}{\sqrt{s\pi_{i_s}}} \right).$$

7: Stage 2: Compute sRRQR with parameter $f \geq 1$ on $\mathbf{V}_k^T \mathbf{S} \mathbf{D}$ to obtain $\mathbf{\Pi}_1 \in \mathbb{R}^{s \times k}$

8: Form S with the first k columns of $\mathbf{\Pi}$: $\mathbf{\Pi}_1 = \mathbf{\Pi}(:, 1:k)$.

9: **end procedure**

5.2. Analysis of the sampling. We now derive a result on the D-optimal criterion if Algorithm 5.1 is used to select the sensors. The result gives insight into the minimal number of samples s .

THEOREM 5.1 (Random sampling). *Let $\epsilon, \delta \in (0, 1)$ be user-specified parameters and suppose $s \geq 4k\epsilon^{-2} \log(k/\delta)$. Define $\mathbf{C}_{\text{lev}} = \mathbf{A} \mathbf{S} = \mathbf{A}(:, S_{\text{lev}})$ and $\mathbf{C}_{\text{hyb}} = \mathbf{A} \mathbf{S} \mathbf{\Pi}_1 = \mathbf{A}(:, S_{\text{hyb}})$ as the unweighted columns generated using Algorithm 5.1. Then with probability at least $1 - \delta$, for the*

$$\Psi(\mathbf{\Sigma}_k / (q_f^U(m, s, k))) \leq \phi(S_{\text{hyb}}) \leq \phi(S_{\text{lev}}),$$

where $q_f^U(m, s, k) \equiv q_f(s, k) \sqrt{(2m/s(1-\epsilon))}$.

Proof. See Section 7.3 □

Since \mathbf{C}_{lev} chooses $s \geq k$ columns, the upper bound of $\Psi(\mathbf{\Sigma}_k)$ no longer holds for $\phi(S_{\text{lev}})$, but it is true that $\phi(S_{\text{hyb}}) \leq \Psi(\mathbf{\Sigma}_k)$.

5.3. Summary of computational costs. Let us look at the savings in flops achieved via randomized sampling instead of running a QR factorization. Computing the sampling probabilities $\{\pi_j\}_{j=1}^m$ requires one pass over \mathbf{V}_k , and costs $O(mk)$ flops. Sampling and forming the selection matrix requires $O(s)$ flops. The cost of the second stage requires an additional pivoted QR factorization performed on an $k \times s$ matrix.

This takes $O(k^2 s \log_f s)$ flops (sRRQR) or $O(k^2 s)$ flops (QRCP) depending on the algorithm used.

6. Data completion. Suppose we are given a limited set of measurements $\mathbf{S}^\top \mathbf{d} \in \mathbb{R}^k$, that collects data at sensors as determined by the selection operator \mathbf{S} . We want to “complete” the measurements to provide the data at all the candidate measurement locations. The completed data can then be used to solve an inverse problem by computing the MAP estimate, or using another inversion technique.

To this end, suppose we are given the right singular vectors \mathbf{V}_k of the preconditioned operator \mathbf{A} . We further assume that $\mathbf{S}^\top \mathbf{V}_k$ is invertible, and we can define the oblique projector $\mathcal{P} \equiv \mathbf{V}_k (\mathbf{S}^\top \mathbf{V}_k)^{-1} \mathbf{S}^\top$ (notice $\mathcal{P}^2 = \mathcal{P}$, so it is idempotent). We propose the following approximation to \mathbf{d} through the formula

$$(6.1) \quad \mathcal{P} \mathbf{d} = \mathbf{V}_k (\mathbf{S}^\top \mathbf{V}_k)^{-1} (\mathbf{S}^\top \mathbf{d}).$$

Notice that in the expression above we only select data at $\mathbf{S}^\top \mathbf{d}$. This approach uses a judicious combination of the forward operator, prior and noise covariance matrices to generate the basis \mathbf{V}_k . The projector \mathcal{P} is an interpolatory projector [47, Definition 3.1] and has the interpolatory property $\mathbf{S}^\top \mathcal{P} \mathbf{d} = \mathbf{S}^\top \mathbf{d}$. This implies that $\mathcal{P} \mathbf{d}$ matches \mathbf{d} *exactly* (in exact arithmetic) at the indices determined by \mathbf{S} . A similar approach has been used in model reduction and is called the Discrete Empirical Interpolation Method (DEIM) approach [16]. We call our approach Bayesian-Discrete Empirical Interpolation Method (B-DEIM), to recognize the fact that the basis arises from the forward operator preconditioned by the square roots of the noise and the prior covariance matrices. Note that this approach gives an inexpensive way to complete the data (assuming the singular vectors \mathbf{V}_k are available) without having to solve the inverse problem explicitly.

We now derive a result on the squared absolute error in the completed data.

THEOREM 6.1 (B-DEIM error). *Let $\mathbf{\Gamma}_{\text{noise}} = \eta^2 \mathbf{I}$ and let $1 \leq k < m$. Let $\mathcal{P} \mathbf{d}$ be the completed data as in (6.1). The absolute error in the completed data satisfies*

$$\mathbb{E}_{\mathbf{d}} \left[\left\| (\mathbf{I} - \mathcal{P}) \mathbf{d} \right\|_{\mathbf{\Gamma}_{\text{noise}}^{-1}} \right] \leq \|(\mathbf{S}^\top \mathbf{V}_k)^{-1}\|_2 \left[\|\mathbf{\Sigma}_\perp\|_F + \|\mathbf{\Sigma}_\perp\|_2 \|\boldsymbol{\mu}_{\text{pr}}\|_{\mathbf{\Gamma}_{\text{pr}}^{-1}} + \sqrt{m-k} \right].$$

The expectation is taken over the data, with density $\pi(\mathbf{d})$.

Proof. See Section 7.4. □

We now discuss an interpretation of this theorem. The absolute error in the completed data is small, in expectation, if the singular values in $\mathbf{\Sigma}_\perp$ decay rapidly, and the amplification factor $\|(\mathbf{S}^\top \mathbf{V}_k)^{-1}\|_2$ is small. If sRRQR is used with parameter $f \geq 1$ to determine the selection operator \mathbf{S} as in Algorithm 3.1, then the bound takes the form

$$(6.2) \quad \mathbb{E}_{\mathbf{d}} \left[\left\| (\mathbf{I} - \mathcal{P}) \mathbf{d} \right\|_{\mathbf{\Gamma}_{\text{noise}}^{-1}} \right] \leq q_f(m, k) \left[\|\mathbf{\Sigma}_\perp\|_F + \|\mathbf{\Sigma}_\perp\|_2 \|\boldsymbol{\mu}_{\text{pr}}\|_{\mathbf{\Gamma}_{\text{pr}}^{-1}} + \sqrt{m-k} \right].$$

It should also be noted that the completed data $\mathcal{P} \mathbf{d}$ has a noise covariance matrix that is no longer uncorrelated; in particular the noise covariance is changed to $\mathcal{P} \mathbf{\Gamma}_{\text{noise}} \mathcal{P}^\top = \eta^2 \mathbf{V}_k (\mathbf{S}^\top \mathbf{V}_k)^{-1} (\mathbf{S}^\top \mathbf{V}_k)^{-\top} \mathbf{V}_k^\top$.

Approximate MAP estimate. The completed data $\mathcal{P} \mathbf{d}$ can be used to define an approximate MAP point

$$\hat{\mathbf{m}}_{\text{post}} \equiv \mathbf{\Gamma}_{\text{post}} (\mathbf{F}^\top (\mathbf{\Gamma}_{\text{noise}}^{-1} \mathcal{P} \mathbf{d}) + \mathbf{\Gamma}_{\text{pr}}^{-1} \boldsymbol{\mu}_{\text{pr}}).$$

The following corollary quantifies the error in the approximate MAP point, which shows that the absolute error in the MAP point has the same upper bound as that of the absolute error in the completed data.

COROLLARY 6.2. *The error in the MAP point in the $\|\cdot\|_{\Gamma_{\text{pr}}^{-1}}$ norm computed using the B-DEIM approach satisfies*

$$\mathbb{E}_{\mathbf{d}} \left[\|\widehat{\mathbf{m}}_{\text{post}} - \mathbf{m}_{\text{post}}\|_{\Gamma_{\text{pr}}^{-1}} \right] \leq q_f(m, k) \left[\|\boldsymbol{\Sigma}_{\perp}\|_F + \|\boldsymbol{\Sigma}_{\perp}\|_2 \|\boldsymbol{\mu}_{\text{pr}}\|_{\Gamma_{\text{pr}}^{-1}} + \sqrt{m-k} \right].$$

Proof. See Section 7.4. \square

7. Proofs. This section collects the proofs from various points in this article. Each subsection is dedicated to covering the proofs from a specific section. Some additional background in Appendix A might help in understanding the proofs.

7.1. Proofs of Section 3.

Proof of Theorem 3.2. Compute the pivoted QR factorization of \mathbf{V}_k^{T} as in (3.2). By assumption, $\mathbf{V}_{11} \in \mathbb{R}^{k \times k}$ is nonsingular. Similarly partition $\mathbf{A}\boldsymbol{\Pi} = \begin{bmatrix} \mathbf{C} & \mathbf{T} \end{bmatrix}$. Write the matrix \mathbf{C} as

$$\mathbf{C} = \mathbf{A}\boldsymbol{\Pi}_1 = \mathbf{U}\boldsymbol{\Sigma}\mathbf{V}^{\text{T}}\boldsymbol{\Pi}_1 = \mathbf{U} \begin{bmatrix} \boldsymbol{\Sigma}_k \mathbf{V}_k^{\text{T}} \boldsymbol{\Pi}_1 \\ \boldsymbol{\Sigma}_{\perp} \mathbf{V}_{\perp}^{\text{T}} \boldsymbol{\Pi}_1 \end{bmatrix} = \mathbf{U} \begin{bmatrix} \boldsymbol{\Sigma}_k \mathbf{V}_{11} \\ * \end{bmatrix}.$$

Multiplication by an orthogonal matrix does not change the singular values, so

$$\sigma_j(\mathbf{C}) = \sigma_j \left(\begin{bmatrix} \boldsymbol{\Sigma}_k \mathbf{V}_{11} \\ * \end{bmatrix} \right) \geq \sigma_j(\boldsymbol{\Sigma}_k \mathbf{V}_{11}) \quad 1 \leq j \leq k.$$

We have used the fact that the singular values of a submatrix are smaller than the singular values of the matrix in which it is contained. Next, write $\boldsymbol{\Sigma}_k = \boldsymbol{\Sigma}_k \mathbf{V}_{11} \mathbf{V}_{11}^{-1}$, and apply the singular value inequalities [6, Problem III.6.2.]

$$\sigma_j(\boldsymbol{\Sigma}_k) \leq \sigma_j(\boldsymbol{\Sigma}_k \mathbf{V}_{11}) \|\mathbf{V}_{11}^{-1}\|_2, \quad 1 \leq j \leq k.$$

Combine with the previous inequality to get

$$\frac{\sigma_j(\mathbf{A})}{\|\mathbf{V}_{11}^{-1}\|_2} \leq \sigma_j(\mathbf{C}) \leq \sigma_j(\mathbf{A}), \quad 1 \leq j \leq k.$$

Here $\sigma_j(\mathbf{A}) = \sigma_j(\boldsymbol{\Sigma}_k)$ are the singular values of \mathbf{A} . The upper bound follows from applying the singular value inequality directly to \mathbf{C} . The desired bound follows from the properties of the logdet. \square

7.2. Proofs of Section 4.

Proof of Theorem 4.1. Only the first inequality needs to be proven, since the rest follows from Theorem 3.2. We first prove that \mathbf{Y} has at least rank k with probability 1 by deriving lower bounds for its singular values.

Given the partitioned SVD of \mathbf{A} (2.1), we can write

$$\mathbf{Y} = \boldsymbol{\Omega}\mathbf{A} = [(\boldsymbol{\Omega}\mathbf{U}_k)\boldsymbol{\Sigma}_k \quad (\boldsymbol{\Omega}\mathbf{U}_{\perp})\boldsymbol{\Sigma}_{\perp}] \mathbf{V}^{\text{T}}.$$

The matrix $\boldsymbol{\Omega}\mathbf{U}_k \in \mathbb{R}^{d \times k}$ has the same distribution as a $d \times k$ Gaussian random matrix with independent entries drawn from $\mathcal{N}(0, 1/d)$, since the Gaussian distribution is

rotationally invariant. Therefore, this matrix has full column rank with probability 1, so it has a left multiplicative inverse. From $\Sigma_k = (\Omega \mathbf{U}_k)^\dagger (\Omega \mathbf{U}_k) \Sigma_k$, we have

$$\sigma_j(\mathbf{Y}) \geq \sigma_j((\Omega \mathbf{U}_k) \Sigma_k) \geq \frac{\sigma_j(\Sigma_k)}{\|(\Omega \mathbf{U}_k)^\dagger\|_2} = \frac{\sigma_j(\mathbf{A})}{\|(\Omega \mathbf{U}_k)^\dagger\|_2} \quad 1 \leq j \leq k.$$

Since $\text{rank}(\mathbf{A}) \geq k$, this shows $\text{rank}(\mathbf{Y}) \geq k$ with probability 1. We can then apply sRRQR on \mathbf{Y} with parameter $f \geq 1$. Then

$$\mathbf{Y} [\Pi_1 \quad \Pi_2] = [\mathbf{Q}_1 \quad \mathbf{Q}_2] \begin{bmatrix} \mathbf{R}_{11} & \mathbf{R}_{12} \\ & \mathbf{R}_{22} \end{bmatrix}.$$

By the guarantees of sRRQR $\sigma_j(\mathbf{Y}\Pi_1) \geq \sigma_j(\mathbf{Y})/q_f(m, k)$ for $1 \leq j \leq k$. Finally, the singular value inequalities imply $\sigma_j(\mathbf{Y}\Pi_1) \leq \|\Omega\|_2 \sigma_j(\mathbf{A}\Pi_1)$ for $1 \leq j \leq k$. Putting all the intermediate steps together, we get

$$\sigma_j(\mathbf{A}\Pi_1) \geq \frac{\sigma_j(\mathbf{Y}\Pi_1)}{\|\Omega\|_2} \geq \frac{\sigma_j(\mathbf{Y})}{q_f(m, k)\|\Omega\|_2} \geq \frac{\sigma_j(\mathbf{A})}{q_f(m, k)\|\Omega\|_2\|(\Omega \mathbf{U}_k)^\dagger\|_2} \quad 1 \leq j \leq k.$$

By a simple modification of the proof technique of [28, Theorem 5.8], we can show with probability at least $1 - \delta$, $\|\Omega\|_2\|(\Omega \mathbf{U}_k)^\dagger\|_2 \leq C_g$. For completeness, we give the details in Appendix C.3. The bound is completed by plugging in the bound for $\|\Omega\|_2\|(\Omega \mathbf{U}_k)^\dagger\|_2$ and using the properties of the log-determinant. \square

7.3. Proofs of Section 5.

Proof of Theorem 5.1. Since the columns of \mathbf{C}_{hyb} is a subset of those in \mathbf{C}_{lev} , follows that $\mathbf{C}_{\text{hyb}}\mathbf{C}_{\text{hyb}}^\top \preceq \mathbf{C}_{\text{lev}}\mathbf{C}_{\text{lev}}^\top$, so $\phi(S_{\text{hyb}}) \leq \phi(S_{\text{lev}})$. From Theorem 3.2 with the selection operator $\mathbf{S}\Pi_1$, we see that

$$\Psi(\Sigma_k / \|(\mathbf{V}_k^\top \mathbf{S}\Pi_1)^{-1}\|_2) \leq \phi(S_{\text{hyb}}).$$

We then need a lower bound for $\|(\mathbf{V}_k^\top \mathbf{S}\Pi_1)^{-1}\|_2$. Let $\mathbf{D}_1 \in \mathbb{R}^{k \times k}$ be a diagonal matrix such that $\mathbf{S}\mathbf{D}\Pi_1 = \mathbf{S}\Pi_1\mathbf{D}_1$; this diagonal matrix \mathbf{D}_1 is a submatrix of \mathbf{D} corresponding to the entries of Π_1 .

Recall $\widehat{\mathbf{S}} = \mathbf{S}\mathbf{D}\Pi_1$. First, we show $\mathbf{V}_k^\top \widehat{\mathbf{S}}$ is invertible with high probability and derive a bound for $\|(\mathbf{V}_k^\top \widehat{\mathbf{S}})^{-1}\|_2$. From [34, Theorem 6.2], with a probability at least $1 - \delta$, we have $\sigma_k(\mathbf{V}_k^\top \widehat{\mathbf{S}}) \geq \sqrt{1 - \epsilon}$. Applying sRRQR with parameter $f \geq 1$, we have

$$(7.1) \quad \frac{\sigma_k(\mathbf{V}_k^\top \widehat{\mathbf{S}})}{q_f(s, k)} \leq \sigma_k(\mathbf{V}_k^\top \mathbf{S}\mathbf{D}\Pi_1),$$

so that with probability at least $1 - \delta$, $\|(\mathbf{V}_k^\top \widehat{\mathbf{S}})^{-1}\|_2 \leq q_f(s, k)/\sqrt{1 - \epsilon}$. Furthermore, $\|\mathbf{D}_1\|_2 \leq \|\mathbf{D}\|_2 \leq \max_{1 \leq j \leq m} (1/\sqrt{s\pi_j}) \leq \sqrt{(2m/s)}$. Putting these intermediate results together, we have probability at least $1 - \delta$

$$(7.2) \quad \|(\mathbf{V}_k^\top \mathbf{S}\Pi_1)^{-1}\|_2 \leq \|(\mathbf{V}_k^\top \mathbf{S}\mathbf{D}\Pi_1)^{-1}\|_2 \|\mathbf{D}\|_2 \leq q_f^U(m, s, k).$$

We have used $(\mathbf{V}_k^\top \mathbf{S}\Pi_1)^{-1} = \mathbf{D}_1(\mathbf{V}_k^\top \mathbf{S}\Pi_1\mathbf{D}_1)^{-1} = \mathbf{D}_1(\mathbf{V}_k^\top \mathbf{S}\mathbf{D}\Pi_1)^{-1}$ and $\|\mathbf{D}_1\|_2 \leq \|\mathbf{D}\|_2$. This establishes the bound. \square

7.4. Proofs of Section 6.

Proof of Theorem 6.1. From $\mathcal{P}\mathbf{V}_k\mathbf{V}_k^\top = \mathbf{V}_k\mathbf{V}_k^\top$, we have $(\mathbf{I} - \mathcal{P}) = (\mathbf{I} - \mathcal{P})(\mathbf{I} - \mathbf{V}_k\mathbf{V}_k^\top)$. Therefore, using submultiplicativity

$$\begin{aligned} \|(\mathbf{I} - \mathcal{P})\mathbf{d}\|_2 &\leq \|\mathbf{I} - \mathcal{P}\|_2 \|(\mathbf{I} - \mathbf{V}_k\mathbf{V}_k^\top)\mathbf{d}\|_2 \\ &= \|(\mathbf{S}^\top\mathbf{V}_k)^{-1}\|_2 \|(\mathbf{I} - \mathbf{V}_k\mathbf{V}_k^\top)\mathbf{d}\|_2. \end{aligned}$$

In moving from the first equation to the second, we have used [49, Theorem 1] which says $\|\mathbf{I} - \mathcal{P}\|_2 = \|\mathcal{P}\|_2$. The theorem applies since $1 \leq k < m$, so $\mathcal{P} \neq \mathbf{0}, \mathbf{I}$ and, furthermore, $\|\mathcal{P}\|_2 = \|(\mathbf{S}^\top\mathbf{V}_k)^{-1}\|_2$ since the columns of \mathbf{V}_k and \mathbf{S} are orthonormal. Taking expectations

$$(7.3) \quad \mathbb{E}_{\mathbf{d}} [\|(\mathbf{I} - \mathcal{P})\mathbf{d}\|_2^2] \leq \|(\mathbf{S}^\top\mathbf{V}_k)^{-1}\|_2^2 \mathbb{E}_{\mathbf{d}} [\|(\mathbf{I} - \mathbf{V}_k\mathbf{V}_k^\top)\mathbf{d}\|_2^2].$$

Using the tower law of conditional expectations, we get

$$\mathbb{E}_{\mathbf{d}} [\|(\mathbf{I} - \mathbf{V}_k\mathbf{V}_k^\top)\mathbf{d}\|_2^2] = \mathbb{E}_{\mathbf{m}} \left\{ \mathbb{E}_{\mathbf{d}|\mathbf{m}} [\|(\mathbf{I} - \mathbf{V}_k\mathbf{V}_k^\top)\mathbf{d}\|_2^2] \right\}.$$

We tackle the inner expectation first. Note that if $\mathbf{x} \sim \mathcal{N}(\boldsymbol{\mu}, \boldsymbol{\Gamma})$, then

$$(7.4) \quad \mathbb{E}[\|\mathbf{x}\|_2^2] = \text{trace}(\boldsymbol{\Gamma}) + \|\boldsymbol{\mu}\|_2^2.$$

Using $\mathbf{d}|\mathbf{m} \sim \mathcal{N}(\mathbf{F}\mathbf{m}, \boldsymbol{\Gamma}_{\text{noise}})$ and (7.4) we get

$$\begin{aligned} \mathbb{E}_{\mathbf{d}|\mathbf{m}} [\|(\mathbf{I} - \mathbf{V}_k\mathbf{V}_k^\top)\mathbf{d}\|_2^2] &= \text{trace}((\mathbf{I} - \mathbf{V}_k\mathbf{V}_k^\top)\boldsymbol{\Gamma}_{\text{noise}}(\mathbf{I} - \mathbf{V}_k\mathbf{V}_k^\top)) \\ &\quad + \|(\mathbf{I} - \mathbf{V}_k\mathbf{V}_k^\top)\mathbf{F}\mathbf{m}\|_2^2. \end{aligned}$$

Since $\boldsymbol{\Gamma}_{\text{noise}} = \eta^2\mathbf{I}$, and $\mathbf{I} - \mathbf{V}_k\mathbf{V}_k^\top$ is an orthogonal projector, the trace term simplifies to $\eta^2(m - k)$. Therefore,

$$\mathbb{E}_{\mathbf{m}} \left\{ \mathbb{E}_{\mathbf{d}|\mathbf{m}} [\|(\mathbf{I} - \mathbf{V}_k\mathbf{V}_k^\top)\mathbf{d}\|_2^2] \right\} = \eta^2(m - k) + \mathbb{E}_{\mathbf{m}} [\|(\mathbf{I} - \mathbf{V}_k\mathbf{V}_k^\top)\mathbf{F}\mathbf{m}\|_2^2].$$

The expectation can be computed explicitly once again using (7.4) as

$$\begin{aligned} \mathbb{E}_{\mathbf{m}} [\|(\mathbf{I} - \mathbf{V}_k\mathbf{V}_k^\top)\mathbf{F}\mathbf{m}\|_2^2] &= \text{trace}((\mathbf{I} - \mathbf{V}_k\mathbf{V}_k^\top)\mathbf{F}\boldsymbol{\Gamma}_{\text{pr}}\mathbf{F}^\top(\mathbf{I} - \mathbf{V}_k\mathbf{V}_k^\top)) \\ &\quad + \|(\mathbf{I} - \mathbf{V}_k\mathbf{V}_k^\top)\mathbf{F}\boldsymbol{\mu}_{\text{pr}}\|_2^2 \\ &= \eta^2 \text{trace}((\mathbf{I} - \mathbf{V}_k\mathbf{V}_k^\top)\mathbf{A}^\top\mathbf{A}(\mathbf{I} - \mathbf{V}_k\mathbf{V}_k^\top)) \\ &\quad + \eta^2 \|(\mathbf{I} - \mathbf{V}_k\mathbf{V}_k^\top)\mathbf{A}^\top\boldsymbol{\mu}_{\text{pr}}\|_2^2 \\ &\leq \eta^2 \|\boldsymbol{\Sigma}_\perp\|_F^2 + \eta^2 \|\boldsymbol{\Sigma}_\perp\|_2^2 \|\boldsymbol{\mu}_{\text{pr}}\|_{\boldsymbol{\Gamma}_{\text{pr}}^{-1}}^2. \end{aligned}$$

Finally, this gives $\mathbb{E}_{\mathbf{d}} [\|(\mathbf{I} - \mathbf{V}_k\mathbf{V}_k^\top)\mathbf{d}\|_2^2] = \eta^2[\|\boldsymbol{\Sigma}_\perp\|_F^2 + \eta^2\|\boldsymbol{\Sigma}_\perp\|_2^2\|\boldsymbol{\mu}_{\text{pr}}\|_{\boldsymbol{\Gamma}_{\text{pr}}^{-1}}^2 + (m - k)]$. Plug into (7.3). The bound follows by using the Cauchy-Schwartz inequality and subadditivity of square roots. \square

Proof of Corollary 6.2. Simple algebraic manipulations show

$$\begin{aligned} \boldsymbol{\Gamma}_{\text{pr}}^{-1/2}(\mathbf{m}_{\text{post}} - \widehat{\mathbf{m}}_{\text{post}}) &= \eta^{-1}\boldsymbol{\Gamma}_{\text{pr}}^{-1/2}\boldsymbol{\Gamma}_{\text{post}}\mathbf{F}^\top(\eta^{-1}(\mathbf{d} - \mathcal{P}\mathbf{d})) \\ &= (\mathbf{A}\mathbf{A}^\top + \mathbf{I})^{-1}\mathbf{A}[\eta^{-1}(\mathbf{d} - \mathcal{P}\mathbf{d})]. \end{aligned}$$

Apply submultiplicativity and (6.2). The bound follows from $\|(\mathbf{A}\mathbf{A}^\top + \mathbf{I})^{-1}\mathbf{A}\|_2 \leq 1$. \square

8. Experimental results. In this section, we demonstrate numerically the efficacy of proposed methods¹.

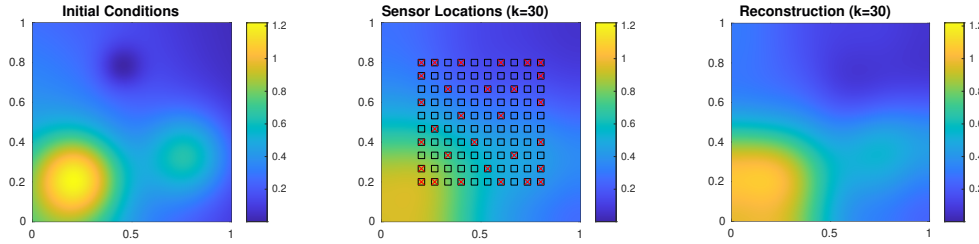


Fig. 1: Problem setup for the Heat problem. The left panel shows the true initial conditions (Franke’s function). The middle panel shows the true state along with the sensor locations as black squares. The red sensors are the ones selected by RandGKS. The right shows the reconstruction from these 30 sensors.

We conducted our numerical experiments on two different test problems from the AIR Tools II package [32] through the IR Tools interface [25].

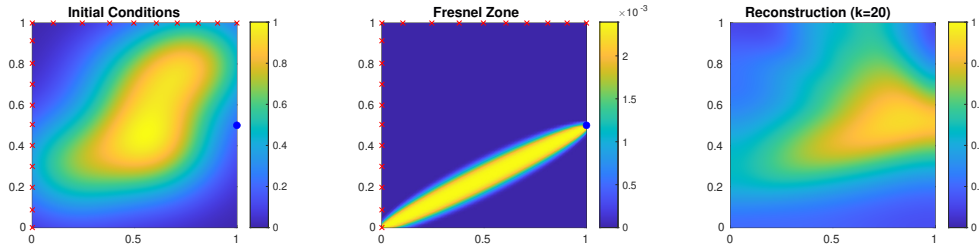


Fig. 2: Problem setup for the seismic tomography problem. The left panel shows the true image along with the blue source on its right boundary. 256 receivers are uniformly placed on the left and top boundaries (a subset of receivers are denoted by red stars). The 20 red locations are selected by RandGKS. A Fresnel zone for one selected source-receiver pair is shown in the middle panel. The right panel contains the reconstruction from the selected sensors.

Application 1: Heat Equation. In this test problem, we consider a 2D heat equation

$$\frac{\partial u}{\partial t} = \Delta u \quad \mathbf{x} \in (0, 1)^2,$$

with homogeneous Neumann boundary conditions. The domain is discretized into a grid of size $65^2 = 4225$ degrees of freedom. The PDE is discretized using linear finite elements. Data is collected at a discrete set of 100 measurement locations at a final time $T = 0.01$ after 100 time steps, and the inverse problem is to recover the initial condition. A plot of the true initial condition, the candidate sensor locations, and the reconstruction is given in Figure 1.

¹Code to reproduce our results is available from <https://github.com/RandomizedOED/css4oed> (see also Appendix E).

Application 2: Seismic travel-time tomography. The goal in this form of tomography is to determine sub-surface attenuation in a domain shown as an $N \times N$ image represented by the flattened vector $\mathbf{x} \in \mathbb{R}^n$ with $n = N^2$ (see Figure 2). The domain is discretized into a grid of size $65^2 = 4225$ with a single source on the right boundary. Furthermore, 256 receivers are located on the left and top boundaries with uniform spacing. The waves are assumed to travel between the source and receiver within the first Fresnel zone, which is shaped as an ellipse with focal points at the source and receiver (see middle panel of Figure 2). The travel time is modeled as an integration of attenuation coefficients over the Fresnel zone. This line integral is discretized using a sensitivity kernel.

We now briefly describe other problem settings. To simulate measurement error, 2% noise is added to the data. We utilize the same prior distributions for both test problems. The prior mean is taken to be zero and the prior covariance matrix is taken to be $\mathbf{\Gamma}_{\text{pr}}^{-1} = \alpha \mathbf{K} \mathbf{M}^{-1} \mathbf{K}$, where \mathbf{K} is a finite element stiffness matrix corresponding to the operator $(-\Delta + \kappa^2)$ with Neumann boundary conditions, and \mathbf{M} is the mass matrix. We use the following values for the parameters, $\kappa^2 = 80$ and $\alpha = 0.1$. A justification for this form of the prior covariance matrix is given in [12]. We report the relative error of the reconstruction in the 2-norm, i.e., $\|\mathbf{m} - \hat{\mathbf{m}}\|_2 / \|\mathbf{m}\|_2$.

8.1. Varying number of sensors. We first consider the performance of the RandGKS algorithm as we increase the number of sensors selected. **RandGKS** is an implementation of Algorithm 3.1 where a randomized SVD algorithm (with $q = 1$ subspace iterations and oversampling $p = 20$) is used to compute the right singular vectors of \mathbf{A} and QRCP is used for computing the pivot indices that determine the sensor placement. We compare RandGKS against the performance of the full operator (Full) in which all sensors are selected.

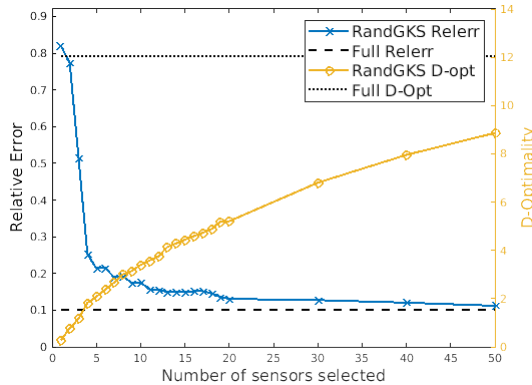


Fig. 3: D-optimality and relative error changes in the RandGKS algorithm with an increasing number of sensors k for the Heat problem. The relative error decreases and the D-optimal criterion increases with increasing k . Notice that we achieve good reconstructions with as few as 20 sensors with respect to the full operator but D-optimality is smaller than that of the full operator.

Figure 3 shows both the relative error and D-optimal criterion as we vary k from 1 to 50 for the Heat problem. On the one hand, moving from left to right, the relative error shows a sharp decrease with an increasing number of sensors $k \leq 20$, and then plateaus which suggest diminishing returns. On the other hand, the D-

optimality increases with increasing number of sensors. The RandGKS method can achieve reasonably good reconstructions with as few as $k = 20$ sensors when compared with Full; however, RandGKS yields a much smaller D-optimal solution compared to Full. Even though there is no improvement in accuracy in terms of relative error, additional information collected from sensors can help reduce the uncertainty (i.e., increased D-optimality).

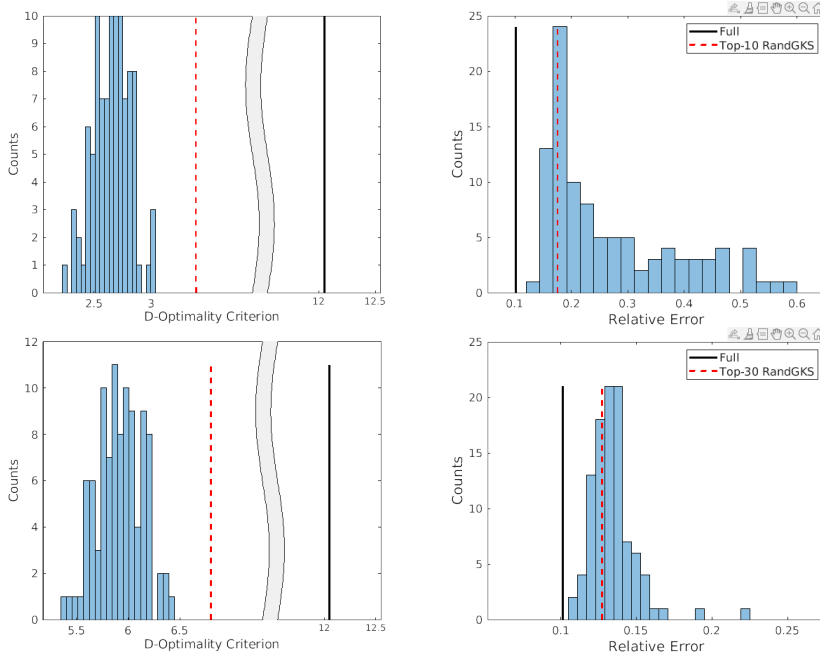


Fig. 4: Evaluating the RandGKS algorithm against random sensor placements in the Heat test problem. We include 100 random sensor selections, with $k = 10$ (top row) and $k = 30$ (bottom row), to plot the D-optimality and relative error histograms. RandGKS always has the highest D-optimality and reasonable relative error for all k .

Next, we investigate two specific choices of k ($k = 10$ and $k = 30$) and compare RandGKS against 100 random sensor placements in Figure 4. The results are displayed in Figure 4 with D-optimality results on the left panel and relative errors on the right; furthermore, the top row corresponds to $k = 10$ and the bottom row corresponds to $k = 30$. The histogram of the random designs is plotted in blue, along with a solid black line indicating Full and a dashed red line indicating RandGKS. We first consider the D-optimal criterion. We can see that RandGKS beats all the random designs in terms of D-optimality but is far from that of the full operators for both $k = 10$ and $k = 30$. Next, we consider the relative errors. Here, RandGKS beats most but not all the random designs. This is expected as we are optimizing only for D-optimality and not reconstruction with our algorithms. The discrepancy with the full operator in terms of relative error is not as drastic as that of D-optimality.

8.2. Comparison of the different methods. In this set of experiments, we compare RandGKS with other methods proposed in this paper and existing methods. We give a brief description of the settings for the algorithms in Appendix D.1.

Table 1: Comparison of the algorithms on Heat ($k = 30$) and Seismic ($k = 50$).

Problem	Algorithm	D-optimality	Relative Error	$\ \mathbf{V}_{11}^{-1}\ _2$	Time
Heat	Full	12.0491	0.1015	—	—
	RandGKS	6.8017	0.1274	5.8193	124.5957 s
	Hybrid	6.6621	0.1194	6.6528	122.8767 s
	Greedy	7.0857	0.1319	∞	1348.8915 s
	RAF	6.6441	0.1263	10.413	41.6364 s
Seismic	Full	13.1040	0.2934	—	—
	RandGKS	5.6962	0.2896	2.9166	1.9811 s
	Hybrid	5.6753	0.2875	10.583	2.1143 s
	Greedy	5.9211	0.2956	4.7025e+07	66.5252 s
	RAF	5.6760	0.2930	15.636	0.6742 s

In Table 1, we display the D-optimal criteria and relative errors for our OED methods and the full operator. This table reports results for both Heat and Seismic problems with $k = 30$ and $k = 50$ sensors, respectively. Note that the results of Full and RandGKS have been previously reported already, but we are including them for comparison. All methods perform similarly in both metrics. We see that for both Heat and Seismic, the Greedy method has the largest D-optimality while Hybrid has the least relative error. The RAF-OED algorithm’s performance is comparable to the other methods, even though it is much cheaper. We also report the value of $\|\mathbf{V}_{11}^{-1}\|_2$ which appears in the denominator of the lower bound from Theorem 3.2. While the Greedy method performed well in our experiments in terms of D-optimality, the value of $\|\mathbf{V}_{11}^{-1}\|_2$ can be large, suggesting that Greedy may select (nearly) dependent columns. Finally, we report the Wall clock times taken by the different methods to perform OED. RAF-OED is clearly the fastest method, with the other randomized algorithms performing reasonably. The Greedy method is the most expensive due to the large number of PDE evaluations involved in its computation. Note that in our implementation, we assumed that the operator \mathbf{A} is not formed explicitly. Further details of the computing environment and timing studies are in Appendix D.4.

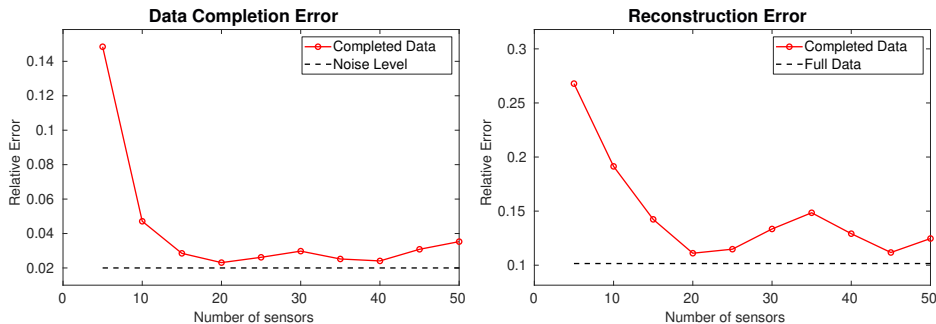


Fig. 5: Results from the data completion experiments for the Heat problem. (left) The error in the completed data with increasing number of sensors, and (right) the reconstruction error using the completed data to compute the MAP estimate.

8.3. Data completion. Next, we consider the performance of the B-DEIM approach to complete the data applied to the Heat problem (see section 6). We increase the number of sensors selected from 5 to 50 using the RandGKS algorithm and plot the relative errors in the completed data (left panel) and reconstruction (right panel) in Figure 5. The relative error for data completion is defined as $\|\mathbf{d} - \mathcal{P}\mathbf{d}\|_2 / \|\mathbf{d}\|_2$, where \mathbf{d} is the data from all sensors, and \mathcal{P} is the B-DEIM projector. The reconstruction error is computed between the MAP estimate obtained by using $\mathcal{P}\mathbf{d}$ as data and the true initial conditions. From the left panel we can see that data completion improves while $k \leq 20$ before stagnating at around 2%. Recall that 2% noise has been added to the data, which naturally limits the data recovery. We see similar trends in the right panel with the MAP estimate. The reconstruction error improves till around 20 sensors before stagnating close to the error obtained by using the full operator. We also report the performance of B-DEIM on the Seismic problem as we increase

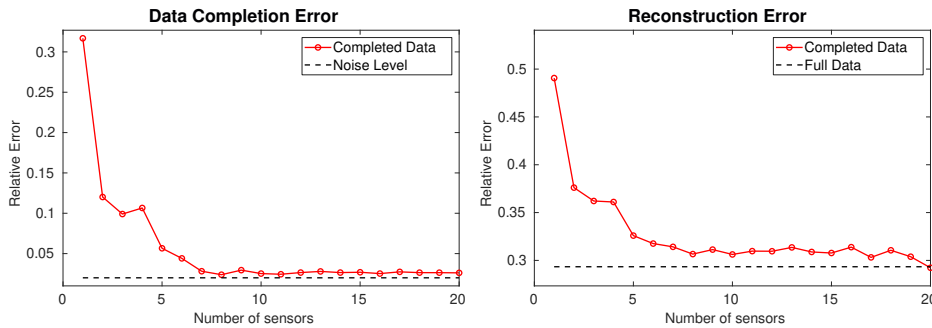


Fig. 6: Data completion experiments for Seismic with (left) error in the completed data versus number of sensors and (right) reconstruction error when the completed data is used to find the MAP point. In both cases the error decreases till 8 sensors and then stagnates.

the number of sensors used from 1 to 20 in Figure 6. We are able to complete the data up to the 2% noise level and recover the MAP estimate with almost the same accuracy as the full operator.

9. Conclusions. This paper presents several algorithms for D-optimal sensor placement in Bayesian inverse problems by leveraging connections to CSSP. We established several algorithms—both deterministic and randomized—with provable guarantees. The algorithms are computationally efficient, easy to implement, and do not require much tuning. Numerical experiments demonstrate the performance of the methods. There are many avenues for future work. First, can we extend this to other criteria, such as A-optimality and goal-oriented? Second, are these techniques applicable to non-linear inverse problems? Third, can we extend the techniques to correlated noise? A possible way forward is to consider the techniques in [23, Section 4.5]. Fourth, based on the connection to CSSP, can other techniques such as volume-sampling and determinantal point processes [5] offer tangible benefits?

Acknowledgments. We would like to thank Ahmed Attia for his help with PyOED and also thank Alen Alexanderian, Wendy Di, Jayanth Jagalur, and Youssef Marzouk for helpful discussions.

Appendix A. Some background results. Let $\mathbf{C}, \mathbf{D} \in \mathbb{R}^{n \times n}$ be symmetric matrices. We say that $\mathbf{C} \preceq \mathbf{D}$ (alternatively, $\mathbf{D} \succeq \mathbf{C}$) if $\mathbf{D} - \mathbf{C}$ is positive semidefinite; see [35, Chapter 7.7] for additional details. By Weyl's inequality, $\lambda_i(\mathbf{C}) \leq \lambda_i(\mathbf{D})$ for $1 \leq i \leq n$, where $\lambda_i(\mathbf{C})$ denote the eigenvalues of \mathbf{C} in decreasing order. For short, we also write $\mathbf{C} \succeq \mathbf{0}$ if \mathbf{C} is symmetric positive semidefinite. We also have $\mathbf{X}\mathbf{C}\mathbf{X}^\top \preceq \mathbf{X}\mathbf{D}\mathbf{X}^\top$ where $\mathbf{X} \in \mathbb{R}^{m \times n}$. If $\mathbf{0} \preceq \mathbf{C} \preceq \mathbf{D}$, then $(\mathbf{I} + \mathbf{C})^{-1} \succeq (\mathbf{I} + \mathbf{D})^{-1}$. Similarly, this also implies [2, Lemma 9]

$$0 \leq \log \det(\mathbf{I} + \mathbf{D}) - \log \det(\mathbf{I} + \mathbf{C}) \leq \log \det(\mathbf{I} + \mathbf{D} - \mathbf{C}).$$

We will also need Sylvester's determinant identity

$$\log \det(\mathbf{I} + \mathbf{A}\mathbf{A}^\top) = \log \det(\mathbf{I} + \mathbf{A}^\top\mathbf{A}).$$

This can be seen for example from the fact that $\mathbf{A}\mathbf{A}^\top$ and $\mathbf{A}^\top\mathbf{A}$ have the same nonzero eigenvalues.

Appendix B. Proof of NP-Hardness. In this section, we give a proof of Proposition 3.1. We restate the decision problem in a slightly different form:

Problem D-optimal sensor placement.

[Instance] Let $\mathbf{A} \in \mathbb{R}^{M \times N}$ with rank at least k , and $\tau \in \mathbb{R}_+$.

[Question] Does there exist a matrix $\mathbf{C} \in \mathbb{R}^{M \times k}$ that contains columns from the matrix \mathbf{A} , i.e., $\mathbf{C} = \mathbf{A}(:, S)$, such that $\phi(S) \geq \tau$?

We give a reduction based on the 'exact cover by 3-sets' (X3C) problem which is known to be NP-complete. This proof technique is based on Civril and Magdon-Ismail [18].

Problem Exact cover by 3-sets (X3C).

Instance A set $\mathcal{S} = \{1, \dots, 3m\}$ and a collection of subsets $\mathcal{K} = \{\mathcal{K}_1, \dots, \mathcal{K}_n\}$ each with cardinality 3.

Question Is there a subset $\mathcal{K}' \subset \mathcal{K}$ that forms an exact cover for \mathcal{S} (Exact cover means every element of \mathcal{S} appears exactly once in \mathcal{K}')?

Before we launch into the proof of Proposition 3.1, we need the following lemma.

LEMMA B.1. *Let $\mathbf{Z} \in \mathbb{R}^{M \times k}$ be a matrix with $k \leq M$ and with column norms 1. Then $\log \det(\mathbf{I} + \mathbf{Z}\mathbf{Z}^\top) \leq k \log 2$ with equality if and only if columns of \mathbf{Z} are orthonormal.*

Proof. Let us denote the columns of $\mathbf{Z} = [\mathbf{z}_1 \ \dots \ \mathbf{z}_k]$ and singular values of \mathbf{Z} as $\sigma_1 \geq \dots \geq \sigma_k \geq 0$. Then $\|\mathbf{Z}\|_F^2 = \sum_{j=1}^k \|\mathbf{z}_j\|_2^2 = \sum_{j=1}^k \sigma_j^2 = k$ and

$$\log \det(\mathbf{I} + \mathbf{Z}\mathbf{Z}^\top) = \log \det(\mathbf{I} + \mathbf{Z}^\top\mathbf{Z}) \leq \sum_{j=1}^k \log(1 + \|\mathbf{z}_j\|_2^2) = k \log 2,$$

where in the first step we used Sylvester's determinant identity and in the second step we used Hadamard's determinant inequality [35, Theorem 7.8.1]. This establishes the inequality. We now consider the case of the equality. If \mathbf{Z} has orthonormal columns, all its singular values are 1, so equality is achieved. To show the converse, consider the equality

$$\log \det(\mathbf{I} + \mathbf{Z}\mathbf{Z}^\top) = \sum_{j=1}^k \log(1 + \sigma_j^2) = k \log 2,$$

which we can rewrite as $\prod_{j=1}^k (1 + \sigma_j^2) = 2^k$ or $\sum_{j=1}^k \log((\sigma_j^2 + 1)/2) = 0$. Together with $\sum_{j=1}^k \sigma_j^2 = k$, we have

$$\sum_{j=1}^k \left[\frac{\sigma_j^2 - 1}{2} - \log((\sigma_j^2 + 1)/2) \right] = 0.$$

Consider the function $g(x) = (x - 1)/2 - \log((x + 1)/2)$. This function is nonnegative and it has a unique global minimizer at $x = 1$ and $g(1) = 0$. This implies that the only solution to $\sum_{j=1}^k g(\sigma_j^2) = 0$ is $\sigma_1 = \dots = \sigma_k = 1$, or \mathbf{Z} has orthonormal columns. \square

We are ready to prove Proposition 3.1. We show that every instance of X3C is true if and only if the corresponding decision problem for D-optimal sensor placement is true. To this end, we construct the matrix $\mathbf{A} \in \mathbb{R}^{3m \times n}$ with entries ($1 \leq i \leq 3m$, $1 \leq j \leq n$)

$$a_{ij} = \begin{cases} \frac{1}{\sqrt{3}} & i \in \mathcal{K}_j \\ 0 & \text{otherwise.} \end{cases}$$

Thus, in this instance of X3C, $M = 3m$, $N = n$, $k = m$, and $\tau = m \log 2$. We note that the columns of \mathbf{A} have norm 1 so Lemma B.1 applies.

From the proof of [18, Theorem 4], the instance of X3C is true if and only there exists a matrix $\hat{\mathbf{C}} \in \mathbb{R}^{3m \times m}$ (containing columns from \mathbf{A} indexed by set \hat{S}) with orthonormal columns. By Lemma B.1, this is equivalent to showing that $\phi(\hat{S}) = \tau = m \log 2$. Therefore, the instance of X3C is true if and only if there is a set \hat{S} with $\phi(\hat{S}) = m \log 2$. This completes the proof.

Appendix C. Alternatives. In Appendix C.1, we give an alternative to the GKS bounds proposed in Section 3.1, and in Appendix C.2 we give some alternative techniques using maximum-volume. In Appendix C.3, we give additional details of the proof of Theorem 4.1.

C.1. Alternatives to the GKS bounds. Sections 3.1 and 3.2 show two different lower bounds for $\phi(S)$. The first is the GKS bounds which can be extended to the top- k singular values as follows. Let the truncated SVD of \mathbf{A} be $\mathbf{U}_k \mathbf{\Sigma}_k \mathbf{V}_k^T$ with $\mathbf{V}_k \in \mathbb{R}^{m \times k}$. Let \mathbf{V}_k be partitioned exactly as (3.2) into

$$\mathbf{V}_k^T [\mathbf{\Pi}_1 \quad \mathbf{\Pi}_2] = [\mathbf{V}_{11} \quad \mathbf{V}_{22}].$$

Now let us denote the $\ell \times \ell$ principal submatrix of \mathbf{V}_{11} as $\mathbf{V}_{11}(1 : \ell, 1 : \ell) = \mathbf{V}_{(\ell, \ell)}$. Then by the GKS bounds we have [26, Theorem 5.5.2],

$$(C.1) \quad \frac{\sigma_j(\mathbf{A})}{\|(\mathbf{V}_{(j,j)})^{-1}\|_2} \leq \sigma_j(\mathbf{C}) \leq \sigma_j(\mathbf{A}), \quad 1 \leq j \leq k.$$

Notice that the block matrix varies for each singular value making it unwieldy to apply for the D-optimal criterion as in Corollary 3.3. Contrast this with the bounds in Theorem 3.2 which gives us

$$(C.2) \quad \frac{\sigma_j(\mathbf{A})}{\|\mathbf{V}_{11}^{-1}\|_2} \leq \sigma_j(\mathbf{C}) \leq \sigma_j(\mathbf{A}), \quad 1 \leq j \leq k.$$

In situations where a tighter lower bound for $\phi(S)$ is desired, one can compare (C.1) and (C.2) for every singular value. Formally, let define

$$d_j = 1 / \min \left(\|\mathbf{V}_{(j,j)}^{-1}\|_2, \|\mathbf{V}_{11}^{-1}\|_2 \right) \quad 1 \leq j \leq k$$

and let $\mathbf{D} = \text{diag}(d_1, \dots, d_k) \in \mathbb{R}^{k \times k}$. Then using similar arguments as those in Section 7.1 we get

$$\Psi(\mathbf{\Sigma}_k \mathbf{D}) \leq \phi(S) \leq \phi(S^{\text{opt}}) \leq \Psi(\mathbf{\Sigma}_k) \leq \phi([m]).$$

C.2. Maximum volume-based approaches. The connection to maximum volume suggests some alternative approaches. That is, we should select columns of $\widehat{\mathbf{A}} \equiv [\mathbf{I} \ \mathbf{A}^\top]^\top$, rather than directly select columns of \mathbf{A} . First notice that the singular values of $\widehat{\mathbf{A}}$ are related to \mathbf{A} as

$$\sigma_i(\widehat{\mathbf{A}}) = \sqrt{1 + \sigma_i(\mathbf{A})^2} \quad \text{for } 1 \leq i \leq \min\{m, n\}.$$

If we apply sRRQR with parameter $f \geq 1$ to $\widehat{\mathbf{A}}$ then we get a matrix $\widehat{\mathbf{C}}$ with k columns from $\widehat{\mathbf{C}}$ of the form

$$\widehat{\mathbf{C}} = \begin{bmatrix} * \\ \mathbf{C} \end{bmatrix} \in \mathbb{R}^{(n+m) \times k},$$

where \mathbf{C} contains k columns from \mathbf{A} . The block denoted by $*$ is zero except for k rows which contain the $k \times k$ identity matrix. From the sRRQR bounds

$$\frac{\sigma_i(\widehat{\mathbf{A}})}{q_f(m, k)} \leq \sigma_i(\widehat{\mathbf{C}}) \leq \sigma_i(\widehat{\mathbf{A}}) \quad 1 \leq i \leq k.$$

This leads to the bounds

$$\Psi(\mathbf{\Sigma}_k) - 2k \log q_f(m, k) \leq \phi(S) \leq \Psi(\mathbf{\Sigma}_k).$$

That is, we get an additive bound rather than a multiplicative bound. Since the factor $q_f(m, k) \geq 1$, it is easy to see that $\Psi(\mathbf{\Sigma}_k/q_f(m, k)) \geq \Psi(\mathbf{\Sigma}_k) - 2k \log q_f(m, k)$. Therefore, this approach produces a looser upper bound, so we did not investigate this further. We leave it to future work to find approaches that exploit this connection to yield better results.

C.3. Details of the proof of Theorem 4.1. We want to provide details of the statement $\|\mathbf{\Omega}\|_2 \|(\mathbf{U}_k \mathbf{\Omega})^\dagger\|_2 \leq C_g$ with probability at least $1 - \delta$. From [31, Proposition 10.2], $\mathbb{E}[\|\mathbf{\Omega}\|_2] \leq \sqrt{\frac{n}{d}} + 1$. Next, $\|\cdot\|_2$ is a Lipschitz function with Lipschitz constant 1, so by the previous result and [31, Proposition 10.3]

$$\mathbb{P} \left\{ \|\mathbf{\Omega}\|_2 \geq \sqrt{\frac{n}{d}} + 1 + t \right\} \leq e^{-t^2/2}.$$

Set $e^{-t^2/2} = \delta/2$ to obtain $t = \sqrt{2 \log(2/\delta)}$. Therefore, $\|\mathbf{\Omega}\|_2 \leq \sqrt{\frac{n}{d}} + 1 + \sqrt{2 \log(2/\delta)}$ with probability at least $1 - \delta/2$.

Next, we tackle $(\mathbf{\Omega} \mathbf{U}_k)^\dagger$, which we can write as $\mathbf{G} \mathbf{U}_k / \sqrt{d}$ where $\mathbf{G} \in \mathbb{R}^{d \times n}$ is a standard Gaussian matrix (i.i.d. entries from $\mathcal{N}(0, 1)$). By the rotational invariance, $\mathbf{G} \mathbf{U}_k \in \mathbb{R}^{d \times k}$ is also a standard Gaussian random matrix. Therefore, by [31, Proposition 10.4]

$$\mathbb{P} \left\{ \|(\mathbf{\Omega} \mathbf{U}_k)^\dagger\|_2 \geq \sqrt{d} \cdot \frac{e\sqrt{d}}{p+1} \cdot t \right\} \leq t^{-(p+1)}.$$

Once again, set $t^{-(p+1)} = \delta/2$, to get $t = (2/\delta)^{1/(p+1)}$. Therefore, $\|(\mathbf{\Omega}\mathbf{U}_k)^\dagger\|_2 \leq \sqrt{d} \cdot \frac{e\sqrt{d}}{p+1} \cdot (2/\delta)^{1/(p+1)}$ with probability at least $1 - \delta/2$. The proof is completed by a simple union bound argument.

Appendix D. Additional numerical experiments. Additional experiments on the same test problems from Section 8.

D.1. Summary of algorithmic choices. We summarize the choices of problem settings that is used in the comparison of algorithms below.

1. **RandGKS:** We implemented Algorithm 3.1 where a randomized SVD algorithm (with $q = 1$ subspace iterations and oversampling $p = 20$) is used to compute the right singular vectors of \mathbf{A} and QR with column pivoting (QRCP) is used for computing the pivot indices that determine the sensor placement.
2. **Hybrid:** This is the randomized point selection method described in Algorithm 5.1 and then QRCP is used in the second stage of the method to cut down the sampled sensors to exactly the requested number of sensors. The randomized SVD was run with the same parameters as in RandGKS. We use $s = \min\{[k \log k], m\}$, the sampling probabilities $\{\pi_j^\beta\}_{j=1}^m$, where $\pi_j^m = \beta \frac{\tau_j}{k} + (1 - \beta) \frac{1}{m}$ for $1 \leq j \leq m$ and $\beta = 0.9$ in the numerical experiments.
3. **Greedy:** In this approach, we greedily pick columns of \mathbf{A} to maximize the D-optimal criterion. Given indices $I = \{i_1, \dots, i_t\}$ at step t , the method selects an index i_{t+1} from $\{1, \dots, m\} \setminus I$ such that the log determinant of $\mathbf{I} + \mathbf{X}\mathbf{X}^\top$ is maximized, where $\mathbf{X} = [\mathbf{a}_{i_1} \ \dots \ \mathbf{a}_{i_{t+1}}]$. To compute a column norm, we require one matvec with \mathbf{A} to extract the column. Furthermore, this method is expensive compared to the other approaches for large m , as it requires $O(mk)$ matvecs with \mathbf{A} .
4. **RAF:** This is Algorithm 4.1 where QRCP is used for computing the pivot indices directly from the sketch $\mathbf{Y} = \mathbf{\Omega}\mathbf{A}$. We set $p = 20$ as the oversampling parameter.

D.2. Additional results for Seismic Tomography. We repeat the experiments from section 8 for the Seismic tomography problem. The results largely mimic the findings from the Heat problem. Figure 7 shows the performance of the RandGKS algorithm as we increase k . We see diminishing returns in terms of relative errors after 30 sensors, but improving D-optimality (reduction in uncertainty) as we add more sensors. Next we show the performance of RandGKS versus 100 random sensor selections for $k = 10$ and $k = 50$ in Figure 8. RandGKS performs extremely well against the random selections, beating them all in D-optimality and doing extremely well in reconstruction errors as well.

D.3. Additional comparison of algorithms. We expand Table 1 for more values of k for both test problems in Tables 2 and 3. In addition to D-optimality and relative error, we also report $\|\mathbf{V}_{11}^{-1}\|_2$ for both test problems. Recall from Theorem 3.2, that this norm appears in the lower bound for the D-optimal criterion. Greedy has the highest D-optimality but other methods produce comparable results. As is seen from the timing results, Greedy is considerably more expensive.

D.4. Additional run time experiments. We compare the running times of the different algorithms for both the test problems. All our experiments were conducted on a laptop computer with a 12th Gen Intel[®] Core(TM) i7-1280P processor

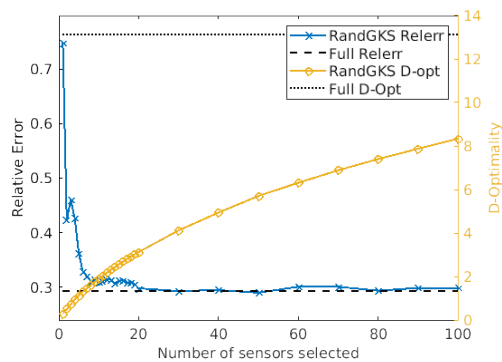


Fig. 7: D-optimal criterion and relative error in the RandGKS algorithm with increasing number of sensors. Relative error stagnates around 30 sensors while D-optimality keeps increasing with more sensors.

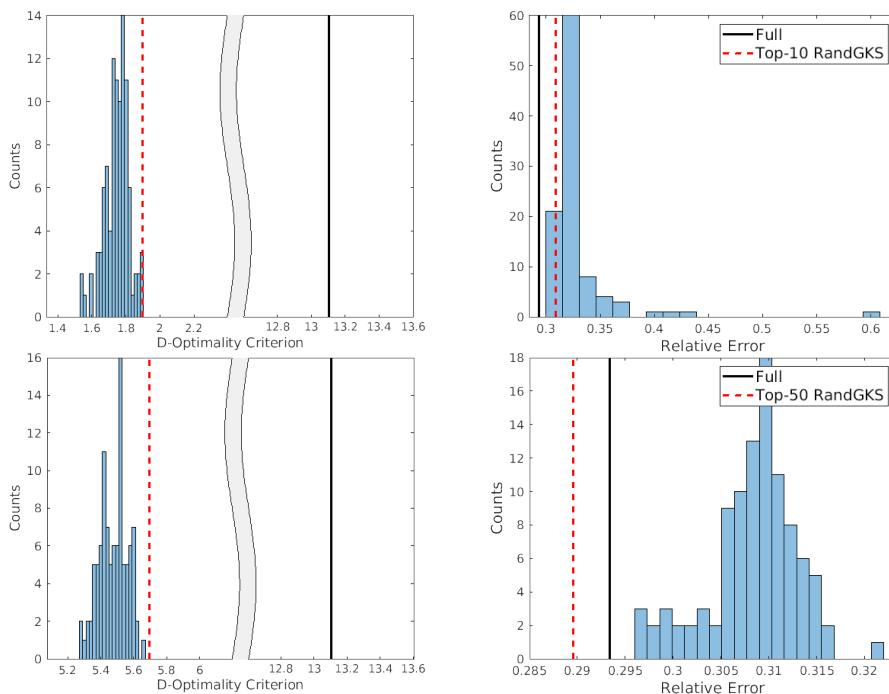


Fig. 8: Evaluating the RandGKS algorithm against random sensor placements in the Seismic problem. 100 random sensor selections, with $k = 10$ or $k = 50$, are used to plot the D-optimality and relative error histograms. RandGKS always has a high D-optimality and reasonable relative error for all k .

and 32 GB of memory using Matlab (version R2023b). We report the wall clock time for different operations in Tables 4 and 5. These timings were collected over 10 different runs and the median time and standard deviation are reported.

From Tables 4 and 5 it clear that Randomized Adjoint-free OED (RAF-OED)

Table 2: Performance of the different algorithms on the Heat test problem.

k	Algorithm	D-optimality	Relative Error	$\ \mathbf{V}_{11}^{-1}\ _2$
—	Full	12.0491	0.1015	—
5	RandGKS	2.0815	0.2144	6.0056
	Hybrid	1.6742	0.4214	8.3106
	Greedy	2.1253	0.2365	18.281
	RAF	1.9467	0.3129	23.73
10	RandGKS	3.3966	0.1758	7.9548
	Hybrid	3.2382	0.2212	10.084
	Greedy	3.5061	0.1768	∞
	RAF	3.3946	0.1721	54.074
20	RandGKS	5.2074	0.1307	5.6349
	Hybrid	5.1778	0.1283	5.7384
	Greedy	5.5779	0.1502	∞
	RAF	5.2897	0.1268	11.251
40	RandGKS	7.9544	0.1204	6.3169
	Hybrid	7.8053	0.1131	15.893
	Greedy	8.3063	0.1298	∞
	RAF	7.7388	0.1075	97.507
50	RandGKS	8.8605	0.1121	7.2188
	Hybrid	8.7376	0.1154	23.067
	Greedy	9.2042	0.1229	∞
	RAF	8.9459	0.1118	1166.3

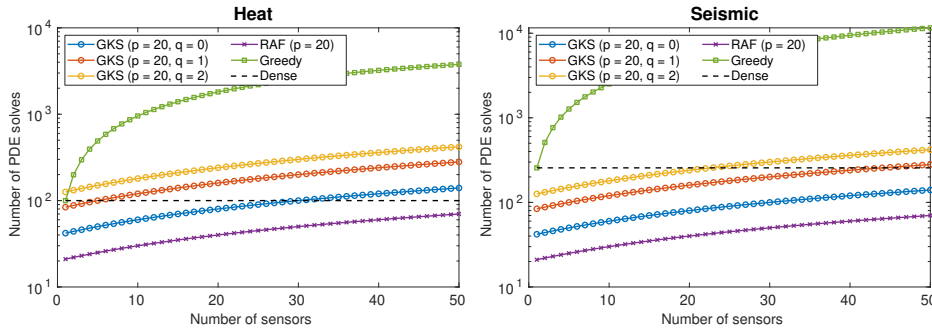


Fig. 9: Scaling the number of PDE solves with the number of sensors selected. Notice that the Greedy algorithm performs a lot more PDE solves, up to two orders of magnitude more, than the randomized methods.

is the fastest method among the four algorithms tested. RandGKS and Hybrid take the next two spots with the Greedy method lagging significantly behind the three randomized methods. The reason for this can be seen from the number of PDE solves incurred by the Greedy method which is an order of magnitude larger than the other

Table 3: Performance of the different algorithms on the Seismic test problem.

k	Algorithm	D-optimality	Relative Error	$\ \mathbf{V}_{11}^{-1}\ _2$
—	Full	13.1040	0.2934	—
10	RandGKS	1.8969	0.3089	5.8451
	Hybrid	1.8398	0.3092	14.004
	Greedy	2.0442	0.4022	2.0046e+05
	RAF	1.8735	0.3097	12.644
20	RandGKS	3.1218	0.2977	4.2127
	Hybrid	3.0885	0.3007	8.6842
	Greedy	3.3450	0.3227	1.8129e+07
	RAF	3.1315	0.3042	20.929
40	RandGKS	4.9363	0.2945	3.1561
	Hybrid	4.9381	0.3034	4.6546
	Greedy	5.1947	0.2952	2.7784e+07
	RAF	4.9676	0.2992	88.5
60	RandGKS	6.3059	0.3006	2.9216
	Hybrid	6.3087	0.3022	5.5387
	Greedy	6.5605	0.2958	4.6921e+09
	RAF	6.3061	0.2961	13.052
80	RandGKS	7.3967	0.2933	7.0063
	Hybrid	7.3979	0.2942	7.9496
	Greedy	7.6556	0.2926	3.2542e+09
	RAF	7.4074	0.2929	558.23

Table 4: Timing results of the different algorithms on the Heat test problem.

k	Algorithm	Matrix-free time median (\pm std)	PDE solves	Dense time median (\pm std)
—	Forward Op	0.4341 (\pm 0.0146)	—	3.90e-05 (\pm 4.95e-05)
—	Adjoint Op	0.4458 (\pm 0.0086)	—	3.85e-05 (\pm 4.09e-05)
10	RandGKS	70.1244 (\pm 2.2287)	120	0.0053 (\pm 0.0023)
	Hybrid	68.9826 (\pm 6.5980)	120	0.0058 (\pm 0.0017)
	Greedy	510.9801 (\pm 4.1313)	955	0.1472 (\pm 0.0301)
	RAF	21.5377 (\pm 1.0847)	30	0.0034 (\pm 0.0010)
30	RandGKS	124.5957 (\pm 1.5266)	200	0.0084 (\pm 0.0009)
	Hybrid	122.876 (\pm 1.1271)	100	0.0078 (\pm 0.0016)
	Greedy	1348.8915 (\pm 21.7416)	2565	0.2843 (\pm 0.0378)
	RAF	41.6364 (\pm 0.2008)	50	0.0034 (\pm 0.0004)

methods.

Figure 9 shows the growth in the number of PDE solves for the different methods as we increase the number of sensors selected k for our test problems. The number of

Table 5: Timing results of the different algorithms on the Seismic test problem.

k	Algorithm	Matrix-free time median (std)	PDE solves	Dense time median (std)
—	Forward Op	0.0056 (\pm 0.0009)	—	7.45e-05 (\pm 1.03e-04)
—	Adjoint Op	0.0048 (\pm 0.0004)	—	3.85e-05 (\pm 4.09e-05)
10	RandGKS	0.6245 (\pm 0.0320)	120	0.0078 (\pm 0.0009)
	Hybrid	0.6194 (\pm 0.0227)	120	0.0086 (\pm 0.0005)
	Greedy	14.1190 (\pm 0.5570)	2515	0.2603 (\pm 0.0078)
	RAF	0.2191 (\pm 0.0049)	30	0.0029 (\pm 0.0003)
50	RandGKS	1.9811 (\pm 0.1418)	280	0.0195 (\pm 0.0027)
	Hybrid	2.1143 (\pm 0.3147)	280	0.0205 (\pm 0.0037)
	Greedy	66.5252 (\pm 3.0533)	11575	2.4353 (\pm 1.0554)
	RAF	0.6742 (\pm 0.0098)	70	0.0075 (\pm 0.0004)

candidate locations, m , is 100 and 256 for the Heat and Seismic problems respectively. The randomized SVD requires $(2q+2)(k+p)$ matvecs for a given oversampling parameter p and subspace iterations q . The Greedy method performs $mk - k(k+1)/2$ solves for a given k . Finally, RAF-OED needs only $k+p$ solves. Notice that only the Greedy method grows as $O(mk)$ whereas all the other methods require only $O(k)$ solves. From Tables 4 and 5 and Figure 9, it is evident that Greedy method is substantially slower.

Since our problems are of modest size, we can simply “densify” the matrices using m PDE solves. This is not possible for larger problems due to the prohibitive memory costs associated with storing the entire forward operator. Even in this setting, we can see from Tables 4 and 5 that our proposed methods outperform the Greedy method. From Figure 9, we can see that the matrix-free versions of the randomized algorithms requires fewer solves than the dense greedy method for small values of k .

Appendix E. Software availability. A software package containing all the scripts and instructions needed to reproduce the numerical experiments in Section 8 and Appendix D can be found in the Github repository². Both Matlab and Python scripts are provided which are compatible with the AIR Tools II/IR Tools [32, 25] and PyOED [17] packages respectively.

REFERENCES

- [1] A. ALEXANDERIAN, *Optimal experimental design for infinite-dimensional Bayesian inverse problems governed by PDEs: A review*, *Inverse Probl.*, 37 (2021), p. 043001.
- [2] A. ALEXANDERIAN AND A. K. SAIBABA, *Efficient D-optimal design of experiments for infinite-dimensional Bayesian linear inverse problems*, *SIAM J. Sci. Comput.*, 40 (2018), pp. A2956–A2985.
- [3] A. ATTIA, S. LEYFFER, AND T. S. MUNSON, *Stochastic learning approach for binary optimization: Application to Bayesian optimal design of experiments*, *SIAM J. Sci. Comput.*, 44 (2022), pp. B395–B427.
- [4] H. AVRON AND C. BOUTSIDIS, *Faster subset selection for matrices and applications*, *SIAM J. Matrix Anal. Appl.*, 34 (2013), pp. 1464–1499.
- [5] A. BELHADJI, R. BARDENET, AND P. CHAINAIS, *A determinantal point process for column subset selection*, *J. Mach. Learn. Res.*, 21 (2020), pp. 8083–8144.

²<https://github.com/RandomizedOED/css4oed>

- [6] R. BHATIA, *Matrix analysis*, vol. 169, Springer Science & Business Media, 2013.
- [7] C. BOUTSIDIS, P. DRINEAS, AND M. W. MAHONEY, *Unsupervised feature selection for the k-means clustering problem*, Advances in neural information processing systems, 22 (2009), <https://doi.org/10.5555/2984093.2984111>.
- [8] C. BOUTSIDIS, M. W. MAHONEY, AND P. DRINEAS, *An improved approximation algorithm for the column subset selection problem*, in Proceedings of the twentieth annual ACM-SIAM symposium on Discrete algorithms, SIAM, 2009, pp. 968–977.
- [9] C. BOUTSIDIS, A. ZOUZIAS, M. W. MAHONEY, AND P. DRINEAS, *Randomized dimensionality reduction for k-means clustering*, IEEE Transactions on Information Theory, 61 (2014), pp. 1045–1062, <https://doi.org/10.1109/TIT.2014.2375327>.
- [10] G. E. BOX AND G. C. TIAO, *Bayesian inference in statistical analysis*, John Wiley & Sons, 1992, <https://doi.org/10.1002/9781118033197>.
- [11] M. E. BROADBENT, M. BROWN, K. PENNER, I. IPSEN, AND R. REHMAN, *Subset selection algorithms: Randomized vs. deterministic*, SIAM undergraduate research online, 3 (2010).
- [12] T. BUI-THANH, O. GHATTAS, J. MARTIN, AND G. STADLER, *A computational framework for infinite-dimensional Bayesian inverse problems part I: The linearized case, with application to global seismic inversion*, SIAM J. Sci. Comput, 35 (2013), pp. A2494–A2523.
- [13] P. BUSINGER AND G. H. GOLUB, *Linear least squares solutions by Householder transformations*, Numer. Math., 7 (1965), pp. 269–276.
- [14] H. CAI, K. HAMM, L. HUANG, AND D. NEEDELL, *Robust cur decomposition: Theory and imaging applications*, SIAM Journal on Imaging Sciences, 14 (2021), pp. 1472–1503, <https://doi.org/10.1137/20M1388322>.
- [15] K. CHALONER AND I. VERDINELLI, *Bayesian experimental design: A review*, Stat. Sci., (1995), pp. 273–304.
- [16] S. CHATURANTABUT AND D. C. SORENSEN, *Nonlinear model reduction via discrete empirical interpolation*, SIAM J. Sci. Comput, 32 (2010), pp. 2737–2764.
- [17] A. CHOWDHARY, S. E. AHMED, AND A. ATTIA, *PyOED: An extensible suite for data assimilation and model-constrained optimal design of experiments*, arXiv preprint arXiv:2301.08336, (2023).
- [18] A. CIVRIL AND M. MAGDON-ISMAIL, *On selecting a maximum volume sub-matrix of a matrix and related problems*, Theor. Comput. Sci., 410 (2009), pp. 4801–4811.
- [19] F. DE HOOG AND R. MATTHEIJ, *Subset selection for matrices*, Linear Algebra and its Applications, 422 (2007), pp. 349–359, <https://doi.org/10.1016/j.laa.2006.08.034>.
- [20] F. DE HOOG AND R. MATTHEIJ, *A note on subset selection for matrices*, Linear algebra and its applications, 434 (2011), pp. 1845–1850, <https://doi.org/10.1016/j.laa.2010.11.053>.
- [21] Y. DONG AND P.-G. MARTINSSON, *Simpler is better: a comparative study of randomized pivoting algorithms for CUR and interpolative decompositions*, Adv. Comput. Math., 49 (2023), p. 66.
- [22] P. DRINEAS, R. KANNAN, AND M. W. MAHONEY, *Fast Monte Carlo algorithms for matrices I: Approximating matrix multiplication*, SIAM J. Comput., 36 (2006), pp. 132–157.
- [23] Z. DRMAC AND A. K. SAIBABA, *The discrete empirical interpolation method: Canonical structure and formulation in weighted inner product spaces*, SIAM J. Matrix Anal. Appl., 39 (2018), pp. 1152–1180.
- [24] J. A. DUERSCH AND M. GU, *Randomized QR with column pivoting*, SIAM J. Sci. Comput, 39 (2017), pp. C263–C291.
- [25] S. GAZZOLA, P. C. HANSEN, AND J. G. NAGY, *IR Tools: a MATLAB package of iterative regularization methods and large-scale test problems*, Numer. Algorithms, 81 (2019), pp. 773–811.
- [26] G. H. GOLUB AND C. F. VAN LOAN, *Matrix computations*, Johns Hopkins Studies in the Mathematical Sciences, Johns Hopkins University Press, Baltimore, MD, fourth ed., 2013.
- [27] S. A. GOREINOV, E. E. TYRTYSHNIKOV, AND N. L. ZAMARASHKIN, *A theory of pseudoskeleton approximations*, Linear algebra and its applications, 261 (1997), pp. 1–21, [https://doi.org/10.1016/S0024-3795\(96\)00301-1](https://doi.org/10.1016/S0024-3795(96)00301-1).
- [28] M. GU, *Subspace iteration randomization and singular value problems*, SIAM Journal on Scientific Computing, 37 (2015), pp. A1139–A1173, <https://doi.org/10.1137/130938700>.
- [29] M. GU AND S. C. EISENSTAT, *Efficient algorithms for computing a strong rank-revealing QR factorization*, SIAM J. Sci. Comput, 17 (1996), pp. 848–869.
- [30] E. HABER, L. HORESH, AND L. TENORIO, *Numerical methods for experimental design of large-scale linear ill-posed inverse problems*, Inverse Probl., 24 (2008), p. 055012.
- [31] N. HALKO, P.-G. MARTINSSON, AND J. A. TROPP, *Finding structure with randomness: Probabilistic algorithms for constructing approximate matrix decompositions*, SIAM Rev., 53 (2011), pp. 217–288.

- [32] P. C. HANSEN AND J. S. JØRGENSEN, *AIR tools II: algebraic iterative reconstruction methods, improved implementation*, Numer. Algorithms, 79 (2018), pp. 107–137.
- [33] E. HERMAN, *Design of Inverse Problems and Surrogate Modeling in Complex Physical Systems*, PhD thesis, North Carolina State University, 2020.
- [34] J. T. HOLODNAK AND I. C. IPSEN, *Randomized approximation of the gram matrix: Exact computation and probabilistic bounds*, SIAM J. Matrix Anal. Appl., 36 (2015), pp. 110–137.
- [35] R. A. HORN AND C. R. JOHNSON, *Matrix analysis*, Cambridge University Press, Cambridge, second ed., 2013.
- [36] X. HUAN, J. JAGALUR, AND Y. MARZOUK, *Optimal experimental design: Formulations and computations*, Acta Numerica, 33 (2024), p. 715–840, <https://doi.org/10.1017/S0962492924000023>.
- [37] J. JAGALUR-MOHAN AND Y. MARZOUK, *Batch greedy maximization of non-submodular functions: Guarantees and applications to experimental design*, J. Mach. Learn. Res., 22 (2021), pp. 11397–11458.
- [38] J. P. KAIPIO AND E. SOMERSALO, *Statistical and Computational Inverse Problems*, Springer, 2005, <https://doi.org/10.1007/b138659>.
- [39] P. MA, M. W. MAHONEY, AND B. YU, *A statistical perspective on algorithmic leveraging*, The Journal of Machine Learning Research, 16 (2015), pp. 861–911.
- [40] M. W. MAHONEY AND P. DRINEAS, *CUR matrix decompositions for improved data analysis*, Proc. Natl. Acad. Sci., 106 (2009), pp. 697–702.
- [41] P.-G. MARTINSSON AND J. A. TROPP, *Randomized numerical linear algebra: Foundations and algorithms*, Acta Numer., 29 (2020), pp. 403–572.
- [42] G. PANTELEEV, M. YAREMCHUK, AND W. E. ROGERS, *Adjoint-free variational data assimilation into a regional wave model*, J. Atmos. Ocean Technol., 32 (2015), pp. 1386–1399.
- [43] F. PUKELSHEIM, *Optimal design of experiments*, vol. 50 of Classics in Applied Mathematics, Society for Industrial and Applied Mathematics (SIAM), Philadelphia, PA, 2006. Reprint of the 1993 original.
- [44] G. QUINTANA-ORTÍ, X. SUN, AND C. H. BISCHOF, *A BLAS-3 version of the QR factorization with column pivoting*, SIAM J. Sci. Comput, 19 (1998), pp. 1486–1494.
- [45] B. J. REICH AND S. K. GHOSH, *Bayesian statistical methods*, Chapman and Hall/CRC, 2019.
- [46] A. K. SAIBABA, *Randomized discrete empirical interpolation method for nonlinear model reduction*, SIAM J. Sci. Comput, 42 (2020), pp. A1582–A1608.
- [47] D. C. SORENSEN AND M. EMBREE, *A DEIM induced CUR factorization*, SIAM J. Sci. Comput, 38 (2016), pp. A1454–A1482.
- [48] A. M. STUART, *Inverse problems: a bayesian perspective*, Acta numerica, 19 (2010), pp. 451–559, <https://doi.org/10.1017/S0962492910000061>.
- [49] D. B. SZYLD, *The many proofs of an identity on the norm of oblique projections*, Numer. Algorithms, 42 (2006), pp. 309–323.
- [50] A. TARANTOLA, *Inverse problem theory and methods for model parameter estimation*, SIAM, 2005, <https://doi.org/10.1137/1.9780898717921>.
- [51] L. TENORIO, F. ANDERSSON, M. DE HOOP, AND P. MA, *Data analysis tools for uncertainty quantification of inverse problems*, Inverse Problems, 27 (2011), p. 045001.
- [52] M. TSITSVERO, S. BARBAROSSA, AND P. DI LORENZO, *Signals on graphs: Uncertainty principle and sampling*, IEEE Transactions on Signal Processing, 64 (2016), pp. 4845–4860, <https://doi.org/10.1109/TSP.2016.2573748>.
- [53] D. UCIŃSKI, *Optimal measurement methods for distributed parameter system identification*, Systems and Control Series, CRC Press, Boca Raton, FL, 2005.
- [54] S. VORONIN AND P.-G. MARTINSSON, *Efficient algorithms for CUR and interpolative matrix decompositions*, Adv. Comput. Math., 43 (2017), pp. 495–516.
- [55] H. WANG, M. YANG, AND J. STUFKEN, *Information-based optimal subdata selection for big data linear regression*, Journal of the American Statistical Association, 114 (2019), pp. 393–405.
- [56] W. J. WELCH, *Algorithmic complexity: three NP-hard problems in computational statistics*, J. Stat. Comput. Simul., 15 (1982), pp. 17–25.
- [57] K. WU, P. CHEN, AND O. GHATTAS, *A fast and scalable computational framework for large-scale high-dimensional Bayesian optimal experimental design*, SIAM-ASA J. Uncertain. Quantif., 11 (2023), pp. 235–261.
- [58] K. WU, P. CHEN, AND O. GHATTAS, *An offline-online decomposition method for efficient linear Bayesian goal-oriented optimal experimental design: Application to optimal sensor placement*, SIAM J. Sci. Comput, 45 (2023), pp. B57–B77.
- [59] W. ZHONG, Y. LIU, AND P. ZENG, *A model-free variable screening method based on leverage score*, Journal of the American Statistical Association, 118 (2023), pp. 135–146.